Paleomagnetic baked-contact tests
in the Mesoproterozoic Sinclair region of Namibia

Jenna M. Hessert
Advisor: David Evans
2nd Reader: Mark Brandon
30 April 2014

A Senior Thesis presented to the faculty of the Department of Geology and Geophysics, Yale University, in partial fulfillment of the Bachelor's Degree.

ABSTRACT

Paleomagnetism of the Sinclair terrane, central Namibia, can help define the Mesoproterozoic apparent polar wander path of the Kalahari craton, during the assembly phase of the Rodinia supercontinent. A previous paleomagnetic study of the region only included blanket demagnetization, but produced preliminary poles that invited further research in the area. The present study is part of a broader investigation analyzing successively older formations within the Sinclair terrane. Within the Sinclair stratigraphy, Barby Formation lavas are unconformably overlain by Guperas Formation sedimentary and volcanic rocks, both of which are intruded by a bimodal dyke suite. Four localities (eight sites) of baked-contact tests of Barby Formation lavas intruded by post-Guperas dykes were sampled. These were thermally demagnetized and then interpreted using principal component analysis. The two western localities yielded positive baked-contact tests, demonstrating primary magnetization in the dykes and pre-dyke magnetization in the lavas. The Barby Formation from these two localities (four sites) yielded mean characteristic remanent magnetizations directed NE with shallow inclination. The central and eastern localities gave interpretable results, but the baked-contact tests were inconclusive. The unbaked Barby Formation host direction from the western localities yielded a virtual geomagnetic pole of ~30N, 85E, distinct from previously published Barby data, but broadly consistent with existing mid-Mesoproterozoic poles from the Kalahari craton. These preliminary results suggest that further investigation of the Barby Formation may yield a robust, primary paleomagnetic pole.

1. INTRODUCTION AND GEOLOGICAL BACKGROUND

In southern Africa, the Kalahari craton is a crucial piece in understanding the configuration of the Rodinia supercontinent that assembled during the Mesoproterozoic. Paleomagnetism of Mesoproterozoic rocks can provide important insights in paleogeographic reconstructions in addition to indicating the behavior of the geomagnetic field at that time. To the west of the Kalahari craton, in southern Namibia, lies the Sinclair terrane (Fig. 1). The Sinclair terrane was affected by the Namaqua-Natal-Maud-Orogeny (NNMO) ca. 1.2-1.0 Ga (Thomas et al., 1994) and is the only really extensive, low-grade terrane within the NNMO that is likely to yield robust paleomagnetic poles.

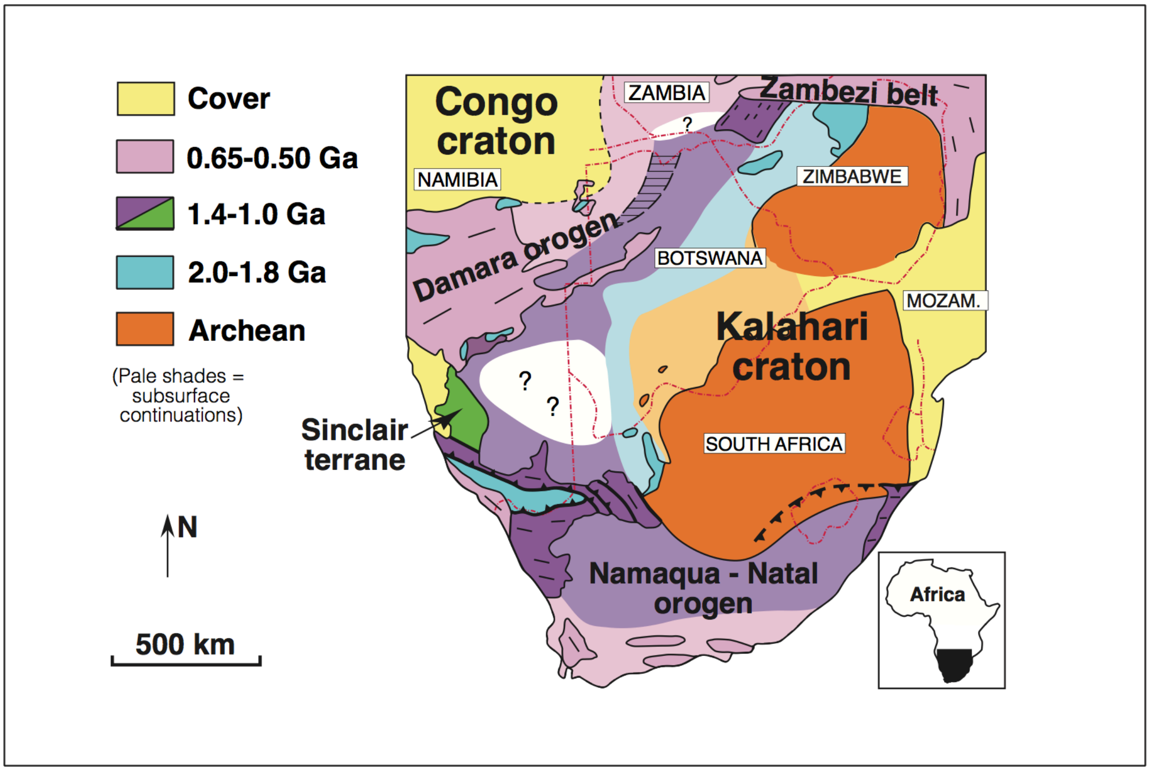

Figure 1. Simplified tectonic map of southern Africa. Modified from Kasbohm et al. (submitted).

The Sinclair Supergroup (Beetz, 1923) is a moderately folded and largely unmetamorphosed volcanic-sedimentary succession that rests on Paleoproterozoic basement of the NNMO. Several cycles of sedimentary and volcanic units are separated by angular unconformities (Fig. 2). The oldest little-metamorphosed sequence comprises Kunjas Formation siliciclastic rocks followed by as much as 3-5 km of Barby Formation mafic volcanic rocks (von Brunn, 1969). The Barby Formation lavas are predominately feldspar-phyric and vary between andesite and basalt in composition, and are associated with subordinate acid lavas and tuffs (Piper, 1975). The formation has been correlated with lavas in the western Awasib Mountains, which are intruded by plutonic rocks dated by U-Pb on zircon at 1215-1220 Ma (Hoal and Heaman, 1995). Because interbasaltic horizons are common, it implies that volcanism was discontinuous (Piper, 1975). Due to extensive faulting in the region (von Brunn, 1969), it is not possible to derive a general stratigraphic sequence within the lavas.

The Guperas Formation, a suite of rocks that includes lava flows and sediments (Martin, 1965), is the next higher unit and is separated from the Barby lavas by an angular unconformity. A bimodal suite of dykes intrudes the Guperas Formation and all older units; the dykes are largely vertical in orientation, thus postdating an episode of moderate deformation of Kunjas, Barby, and Guperas strata. These dykes have recently been dated by U-Pb thermal ionization mass spectrometry (TIMS) on single zircons, at ca. 1105 Ma (S. Bowring, pers. comm. to D. Evans). The Aubures formation was deposited shortly thereafter, as a succession of conglomerates, breccias, red sandstones, and siltstones (Watters, 1974). Mild deformation and block faulting of the Aubures Formation took place contemporaneous with its deposition (Miller, 2008), which is estimated to be ca. 1100-1090 Ma based on concordance of the Aubures paleomagnetic pole with that of the Kalkpunt Formation of the Koras Group in South Africa (Kasbohm et al., submitted). The entire region was then eroded to a flat plane, on which the Nama Group was deposited (Piper, 1975). The Nama Group comprises shallow-water shelf sediments and is predominately arenaceous or argillaceous, as well as including limestone and glacial horizons (Kröner & Rankama, 1972).

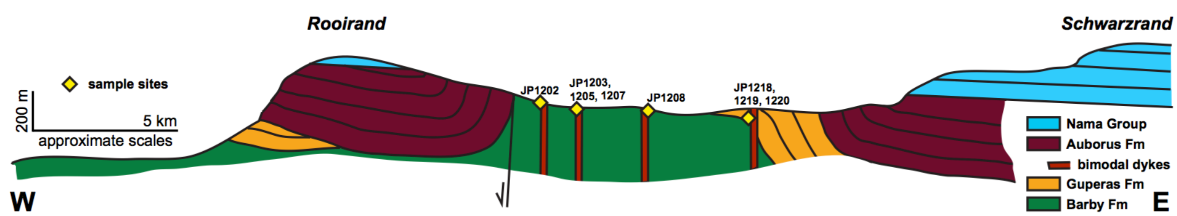

Figure 2. Simplified and schematic cross-section of the Sinclair region, modified from Kasbohm et al. (submitted) to show sample sites from this study. Open fold structures in the Barby Formation are not illustrated for the sake of simplicity.

Piper (1975) was the first to extensively study the Sinclair terrane with paleomagnetic methods and deduce an apparent polar wander path for its constituent rocks. Piper's analysis of the natural remanence magnetism from 19 sites each with 4-7 samples in the Barby Formation yielded a northerly declination and a primarily negative inclination for the characteristic remanence direction, including approximately 5 sites with opposite magnetization that could indicate 2 potential geomagnetic reversals. However, Piper's study was limited due to the technology of the time, and he conducted his analysis using only natural remanent magnetization (NRM) and limited blanket demagnetization. The scatter of directions is very large at this paleolatitude even when considering variations that could have occurred across the region. In addition, Piper's shallow, N-S remanence directions from Barby Formation were very similar to his own data from the overlying Guperas Formation lavas (Piper, 1975), as well as subsequent results from the post-Guperas dykes (Panzik et al., 2013) and Aubures Formation (Kasbohm et al., submitted) (Fig. 3). The possibility thus remained that Piper's (1975) Barby data were magnetically overprinted during Guperas or Aubures times. A more precise study of this region was thus needed to further investigate Piper's results.

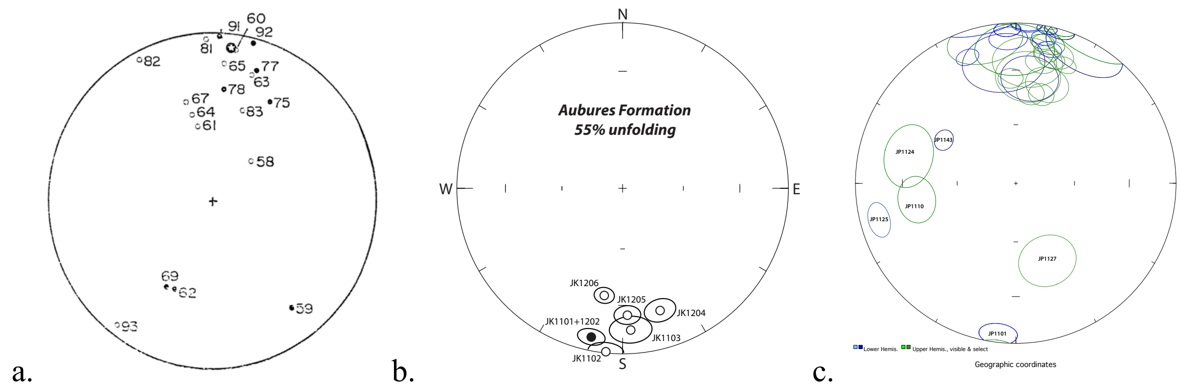

Figure 3. a. Tilt-corrected equal-area stereographic projection of Barby Formation cleaned remanence directions from Piper (1975) b. Kasbohm et al. (submitted) Aubures Fm. with 55% unfolding and c. Panzik et al (in prep.) combined post-Guperas dyke directions.

The present investigation follows the work of Kasbohm et al. (submitted) and Panzik et al. (in prep) of the Aubures and Guperas Formations respectively; the Barby Formation was deposited in an earlier cycle of volcanism than the previous two. Although the present study relies heavily on the data and interpretation of the Guperas paleomagnetism, it is thus the next keystone in reconstructing the Kalahari Craton for its entire paleogeographic history in late Mesoproterozoic time. The present study seeks to determine if Piper's (1975) data record the primary magnetization of the Barby volcanic rocks, and to see if a polar wander path can be determined for Kalahari in the late Mesoproterozoic.

2. PALEOMAGNETIC METHODS

At the field sites, permission was reestablished with the landowners for scouting and sampling from a previous sampling season in 2011. After receiving permission, reconnaissance was performed to pick several sampling localities for the Barby. For each site within each locality, 8 – 26 ten-cm-long core samples were taken. They were obtained using a diamond bit drill and were oriented by magnetic and solar compasses. There was no significant deviation of magnetic declination from the regional average of ~15°W. The four localities where cores were taken are plotted on Figure 4. Cores were taken from the Barby where it was well exposed, as well as along contacts with rhyolitic and mafic dykes, so that baked contact tests (discussed below) could be performed.

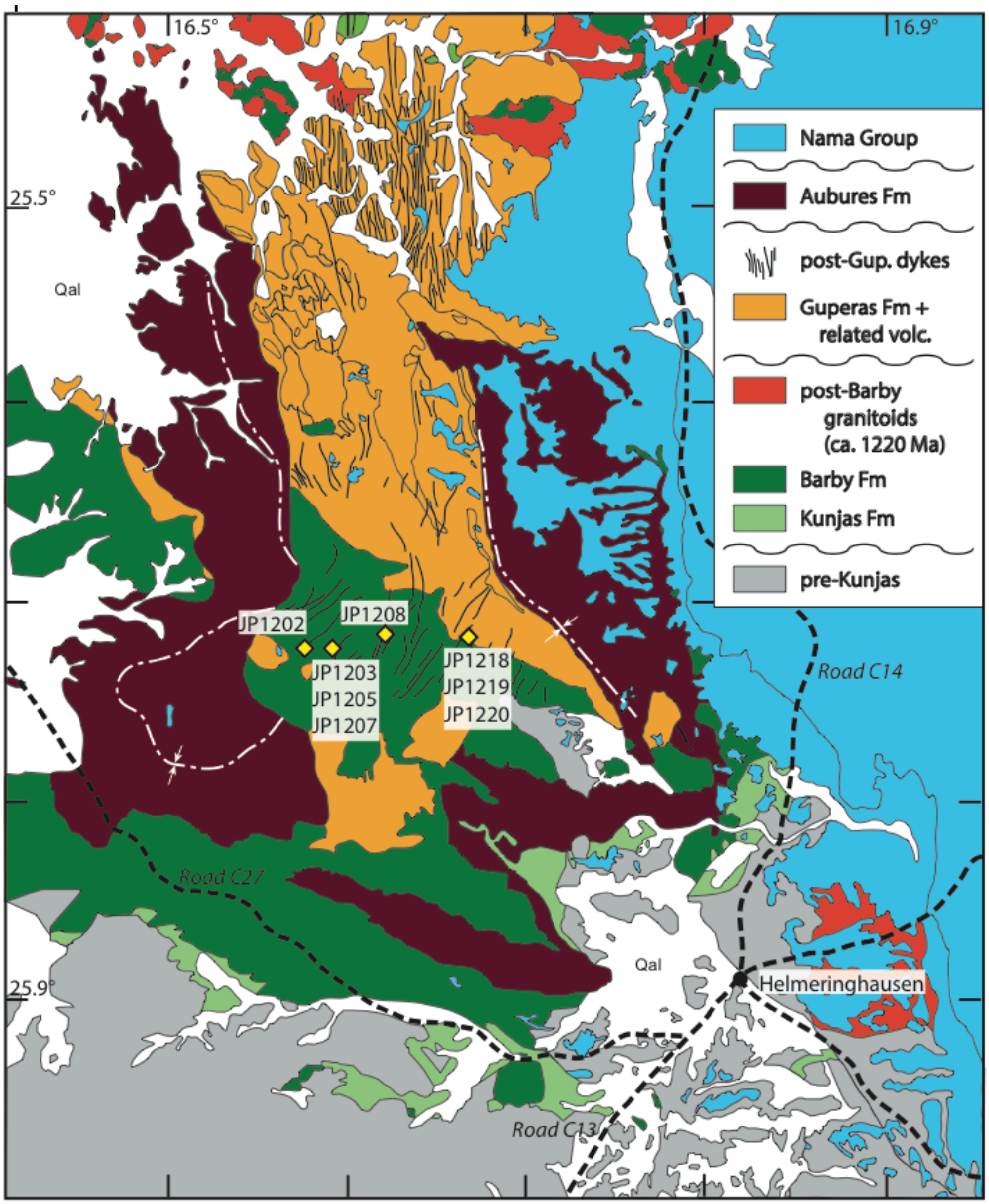

Figure 4. Geologic map of the Sinclair region, south-central Namibia. Sampling sites are denoted by symbols as shown in Fig. 2. Modified from Kasbohm et al., (submitted).

At Yale University, the samples were cut in the rock preparation lab to be cylinders that were approximately 2.2 cm in diameter and 1 cm long. Using a cryogenic DC-SQuID magnetometer, they were analyzed in the Yale Paleomagnetic Facility. This magnetometer contains an automated sample changer (Kirschvink et al., 2008) allowing for rapid acquisition of data in large batches of samples. NRM of all the samples was taken, followed by a low-temperature (liquid nitrogen) demagnetization step to remove any viscous magnetic signals that might be held by large, multidomain magnetite crystals. Then successive steps of high-temperature demagnetization were preformed, decreasing intervals from 100°C in the first few steps, to just 5°C in the highest-temperature steps. All samples reached their Curie point, the temperature step above which the rock loses its magnetism, anywhere from 585°C to 700°C depending on their mineralogy. Using software created by Jones (2002), principal component analysis was used to resolve each sample's magnetic components (Kirschvink, 1980). Additionally, locality means, precision parameters, and 95% confidence limits were calculated using Fisher (1953) statistics.

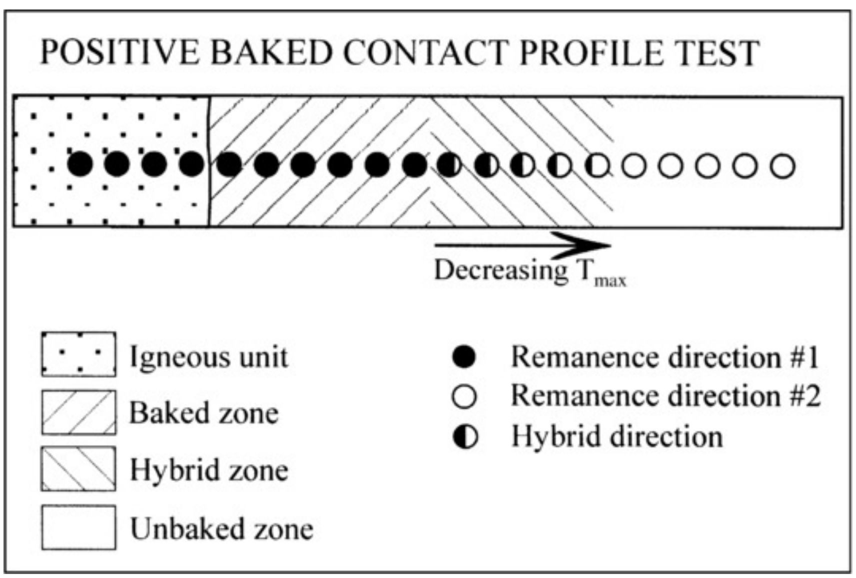

Figure 5. Positive baked-contact test (BCT) profile away from a younger intrusion shown at left. A systematic decrease in the maximum temperature (T_{max}) obtained in the host rocks, as the result of emplacement of igneous unit through a hybrid zone with increasing distance from contact, demonstrates that the younger intrusion imparted a TRM remagnetization of the host. Figure from K. Buchan, 2007.

Baked-contact tests (BCT) were applied to each of the sites where zones of contact between the host rock (the Barby Formation) and the intruding igneous rock (the rhyolitic and mafic dykes) could be identified. The dykes were sampled in the summers of 2011 and in 2012, the results of those tests being used in conjunction with the sampled lavas. Agreement in remanent paleomagnetic direction between the intruding dykes and the adjacent baked host rocks provide confidence that the intruding dyke records a primary magnetization (Butler, 1992; method first employed by Everitt and Clegg, 1962). As the samples from the host rock were taken further away from the baked contact zone, they were expected to show different magnetization than that of the intruding rock, and instead displaying the magnetization of the host formation. Thus if the Barby Formation has a magnetic direction that agrees with the intruding dykes near the baked contact zone, and a different magnetic direction in the unbaked Barby, it will be considered a positive BCT (Butler, 1992). If the test displays uniform directions for the igneous rock, the baked zone, and the unbaked zone, it would be a “failed” BCT, with the sampled rocks recording widespread overprinting that occurred after the younger igneous emplacement.

3. SITE DESCRIPTIONS AND RESULTS

3.1 Western locality JP1202

Near the western edge of the Barby Formation, eight samples (JP1202) were taken near dyke 1101 that was sampled the previous year (Fig. 6). Dyke JP1101, shown in Figure 7, had a south and shallow magnetic direction, with a contact zone transitioning to the Barby direction (that was also sampled in JP1101).

Site JP1202 is sampled 36-49 m away from a NE-striking rhyolitic dyke 18 m in width that had been previously sampled in 2011 (site JP1101). At this site, the Barby Formation consists of fine-grained oxidized basalt with zones of hyaloclastic breccia that dips moderately to the west.

Figure 6. Schematic of site JP1202 and nearby contacts JP1101 and JP1146.

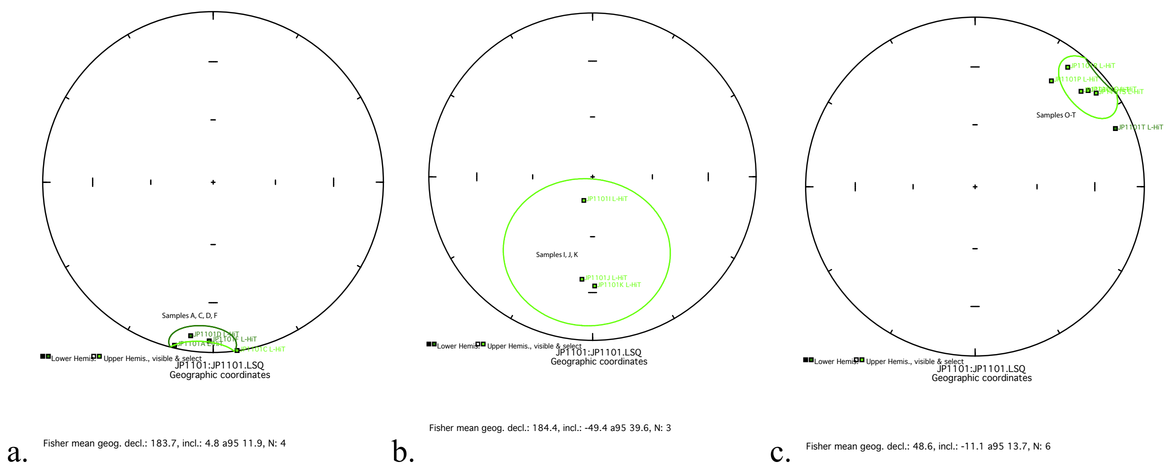

Figure 7. a. JP1101 dyke samples A, C, D, and F (4/6) b. Contact zone containing samples I, J, and K c. Barby Formation lavas samples O-T

The eight samples (A-H) from a massive Barby lava unit all contained hematite, requiring heating to their Curie point of ~700°C. Most showed minor, steady demagnetization until 685°C, when there was an abrupt shift to the origin at 690°C (Fig. 8a). This held true for all eight samples. However, sample H, sampled farthest away from the dyke, showed about 50% demagnetization from 450°C to 555°C, and then clustered again, before the 685-690°C shift to the origin on the remaining 50%. Their magnetization direction stayed constant at NE and shallow until measurements began to scatter about the origin once all magnetization was lost (Fig. 8b). Samples A-E were fitted to a line using all demagnetization steps. Samples F and G were fit to a line for the 200-700°C demagnetization steps, and sample H was fit to a line for the 450-700°C demagnetization steps. All were forced through the origin and always had an angular cone of 95% confidence (A_{95}) of less than 4°.

a. b.

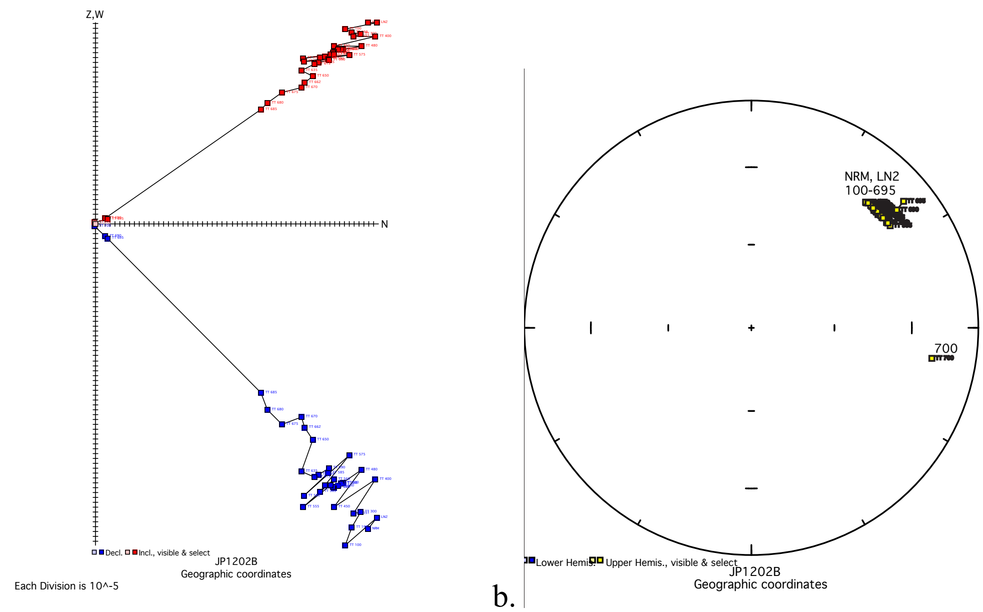

Figure 8. a. Typical Zijderveld diagram for samples from Barby Fm. lavas at JP1202, sample B b. Typical equal area geographic coordinates, JP1202, sample B.

Using all 8 samples, the Fisher mean was calculated at having a declination of 50.7° and inclination of -17.1° and an A_{95} value of 7.6 (Fig. 9a). Tilt-corrected, the magnetic direction becomes NE and shallow, but down with a declination of 052.8° and an inclination of 07.3° (Fig. 9b). It should be noted that in the final demagnetization steps, there was possible movement towards the E-W horizontal in both geographic and core coordinates (owing to the fact that cores at this site had similar orientations). This is most likely due to the alignment of samples in the oven, which contains a very small but nonzero magnetic field (~5nT or less), but could potentially be geologically relevant. Further study would be necessary to confirm this, but the NE and shallow direction is clearly the dominant remanence direction at this site.

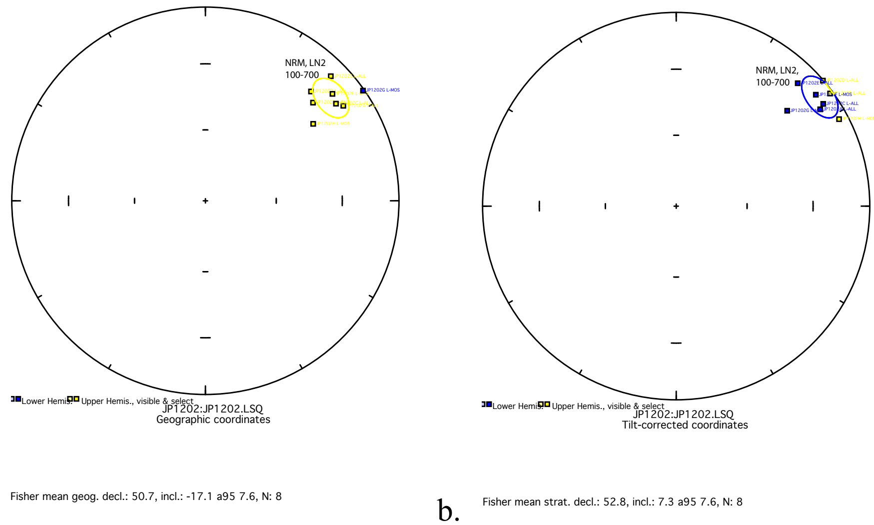

a. b.

Figure 9. Paleomagnetic direction of site JP1202 in (a) geographic coordinates and (b) tilt-corrected coordinates.

3.2. Western localities JP1203, 1205, 1207

Sites JP1203, 1205, and 1207 were slightly to the east of site JP1202 and were sampled in an area containing multiple well-exposed contacts with a rhyolitic and mafic dykes (Fig. 10). JP1203 was sampled 4 m away from the contact with rhyolitic dyke JP1102 (12 m wide), and moving perpendicularly away to the east 26 m. A total of 15 samples (A-O) were collected. The last few samples were slightly south an exposed 4.5 m wide rhyolitic dyke (JP1204), but no dyke exposure could be seen near the end of JP1203. Even further to the north, another rhyolitic dyke was exposed, implying that one or both JP1102 and JP1204 dykes could potentially be part of the same dyke complex.

Figure 10. Schematic of rhyolitic dykes JP1102 and JP1204, and mafic dyke JP1206 with the Barby Fm. sample sites JP1203, JP1205 and JP1207. Orange in the Barby sample sites denotes a dyke direction, while green denotes the Barby, or host rock, direction.

Dyke JP1102 was a pink rhyolitic porphyry dyke w/ white feldspar phenocrysts and was about 12 m wide. From the 8 samples taken, the dyke had a north and up direction, shown in Figure 11.

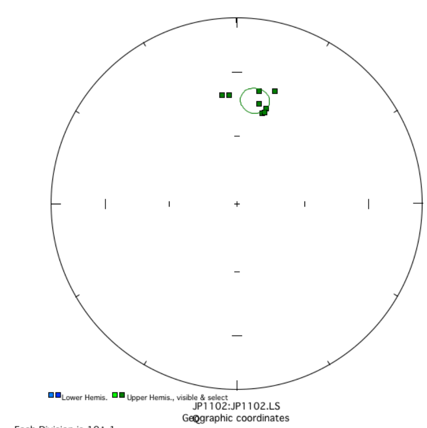

Figure 11. Paleomagnetic direction for rhyolitic dyke collected at site JP1102.

Samples A-E all had one component with steady demagnetization until 700°C (sample E lost its magnetization at 595°C), and northerly direction. Effects of hematite are seen right at the contact from samples A-D. Samples F-I all had a similar component to A-F at lower temperatures. Calculating a Fisher mean from samples A-I (n: 9), gives a north and up directions with a declination of 017.4°, an inclination of -30.9°, and an A_{95} of 5.1° (Fig. 11).

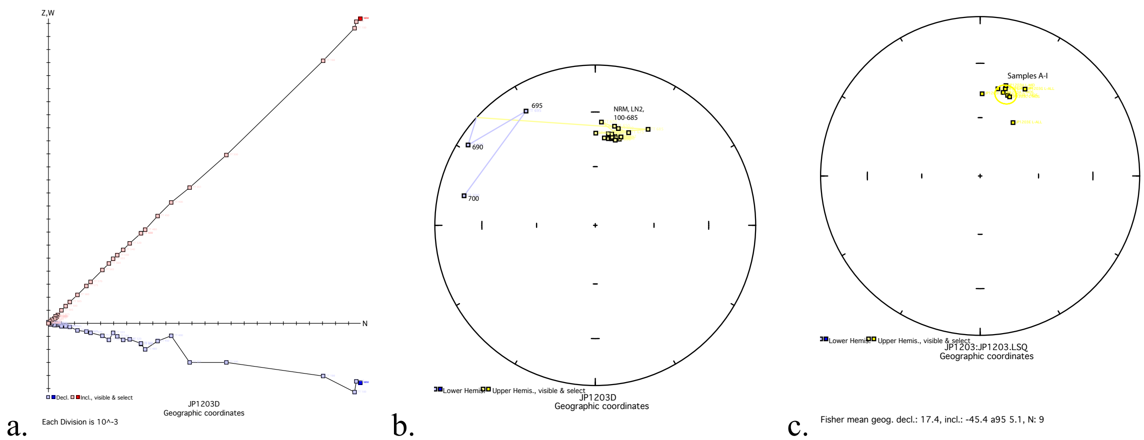

Figure 12. Representative (a) Zijderveld diagram and (b) equal area plot for JP1203D and the (c) geographic means of JP1203 samples A-I.

Samples H, J, and I had multiple magnetic components. The first component being from mid 400°C to 560°C, and the second from 560°C to about 700°C for the second component (Fig. 12a). The magnetization changes from a northeast to east direction during demagnetization (Fig. 12b). From these three samples, the mean geographic declination and inclination is determined to be 062.7° and -7.1°, respectively, with an A_{95} of 16.2° (Fig. 11c). After applying a tilt-correction, the mean becomes 060.9°, 26.3° (Fig. 11d).

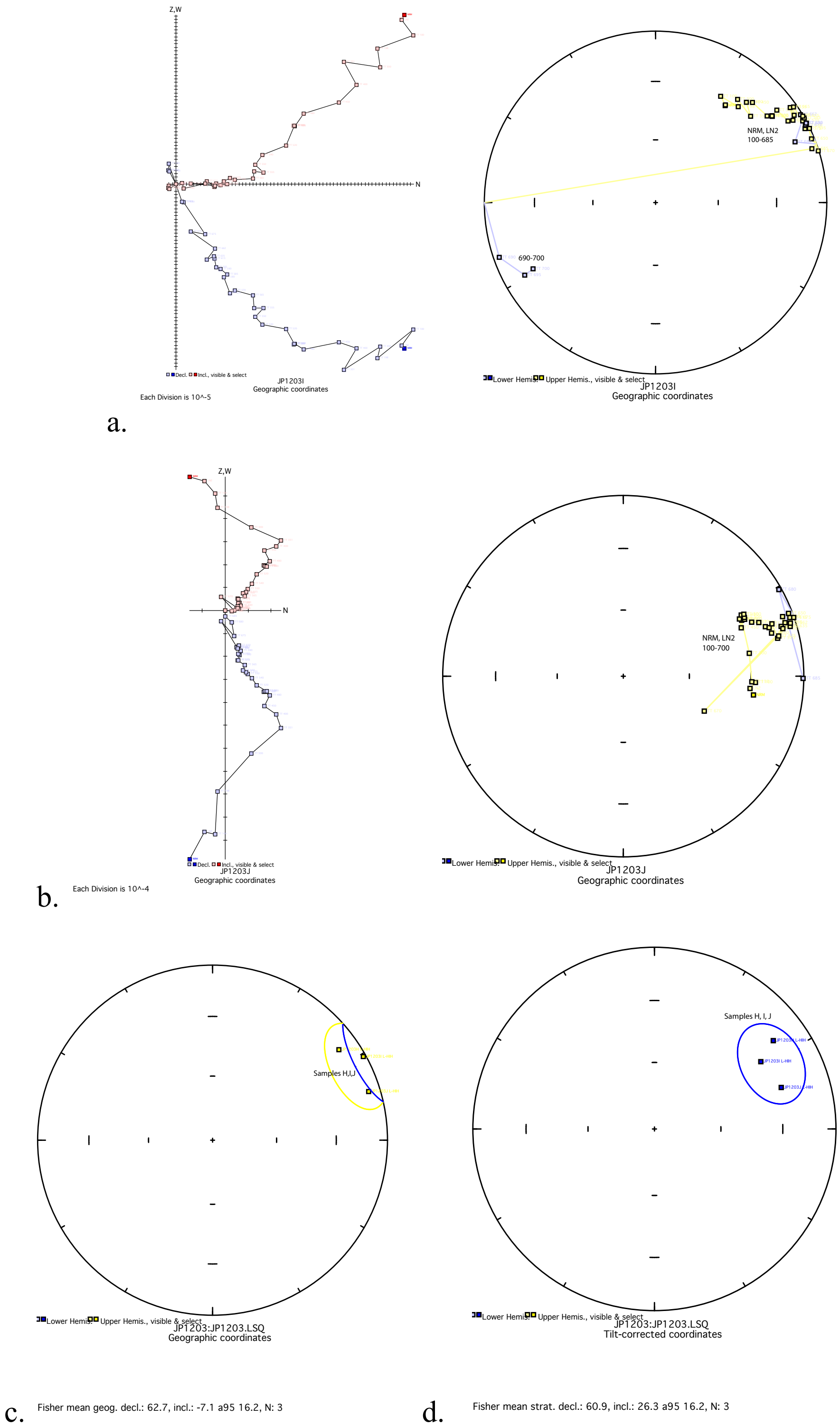

Figure 13. JP1203 samples with magnetic direction representative of the Barby Formation shown by (a) sample I with two components evident, (b) sample J with two components evident, alongside the (c) geographic and (d) tilt-corrected means for samples H, I, and J.

Samples K-O displayed varied components and directions. Samples K and N had characteristics similar to those observed on sample F and G. Three components, which can be seen in Figure 13a, were distinguishable: NRM-400°C, 450°C-560°C, and 565°C-stable end point (SEP). They had a north and up direction, which are similar to the magnetic direction of samples A-I. The magnetization of samples L, M, and O had a south and down direction instead (Fig. 13b). Combining these 5 samples produced a geographic mean magnetic direction with a declination of 002.2°, inclination of -39.9°, and an A_{95} of 16.2 (Fig 14c).

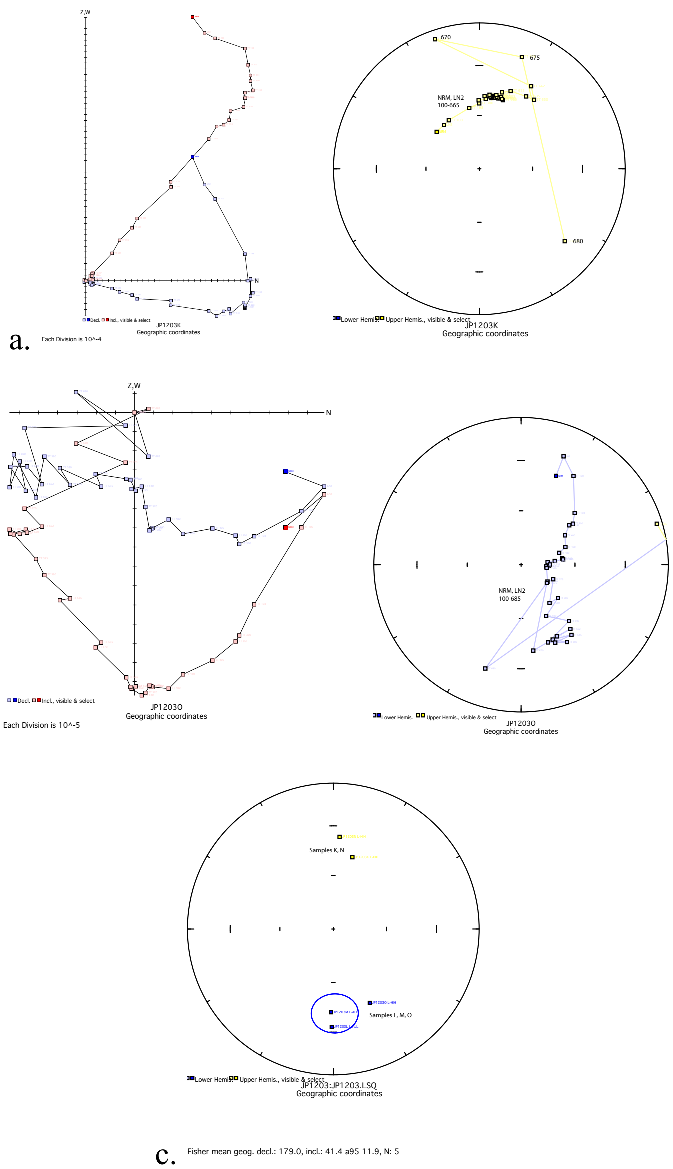

Figure 14. Representative [LEFT] Zijderveld diagrams and [RIGHT] equal area plots for samples (a) K and (b) O in JP1203 and the (c) Geographic Fisher mean for samples K-O.

Site JP1205 was sampled starting less than 1 m to the east of dyke JP1204 (4.5 m wide) and comprised of 17 samples up to 27 m away (Fig.10). The trend of dyke JP1204 is 023°N, 71°E, while the Barby bedding at this site is 184° N, 35°E. The dyke is a rhyolitic porphyry dyke with small, eroded pock marks on its surface. As previously mentioned, it appears this dyke extends further than was observed by the exposed contact and may correlate with the large rhyolite dyke on the northern hillside. From Panzik et al. (in prep.), the sampled dyke has a north and up direction of 014.2°, -42.0° for declination and inclination, respectively (Fig. 15), and is consistent with dyke JP1102.

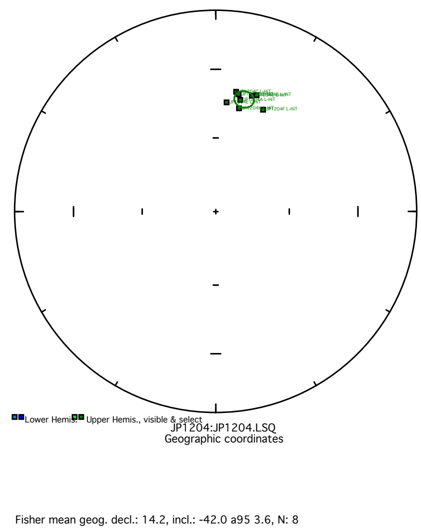

Figure 15. Mean magnetic direction for the rhyolitic dyke JP1204

Samples A-F from JP1205 had either a single component that was north and up, like sample C (Fig. 14a), or were comprised of two components; the lower temperature being north and up, and the higher temperature component being northeast, shallow, and up (Fig. 14b). Calculating the geographic mean from samples A-F (excluding B) results in a north and up direction (011.4°, -39.8°) in agreement with dyke JP1204 (Fig. 14c).

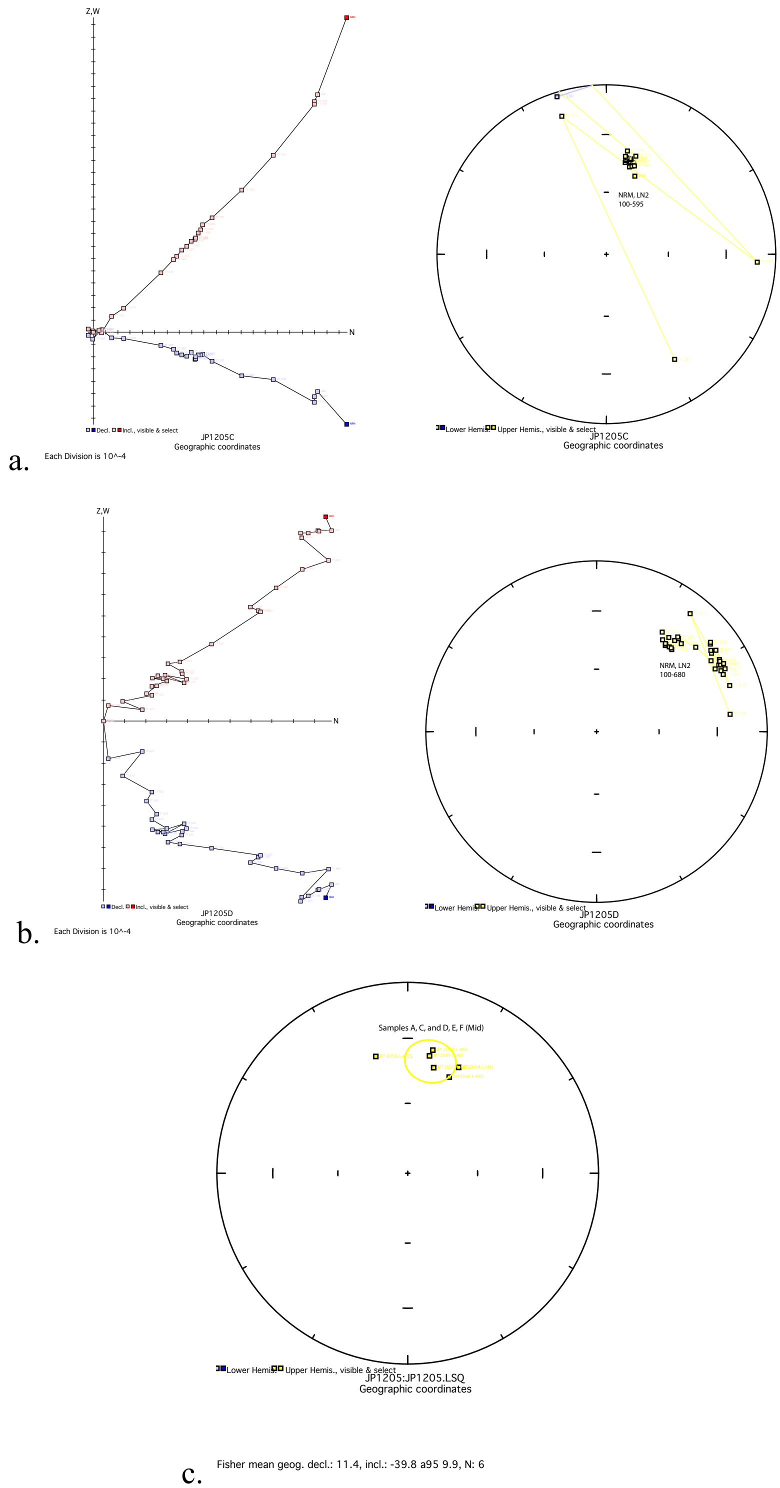

Figure 16. Representative [LEFT] Zijderveld diagrams and [RIGHT] equal area plots for samples (a) C and (b) D in JP1205 with the (c) Geographic mean for samples A,C,D-F (middle temperature component).

The high temperature components of samples D-F in JP1205 were used in computing the Barby direction as well as the remaining samples I-Q. Samples I-Q had most of their demagnetization occur at 670°C, indicating the presence of hematite, and all gave a consistent direction of northeast and shallow (Fig. 17a). The geographic mean of the Barby is 061.4°, -15.5° and tilt-corrected is 061.2°, 17.8° with an A_{95} of 4.8° (Fig. 17b and c).

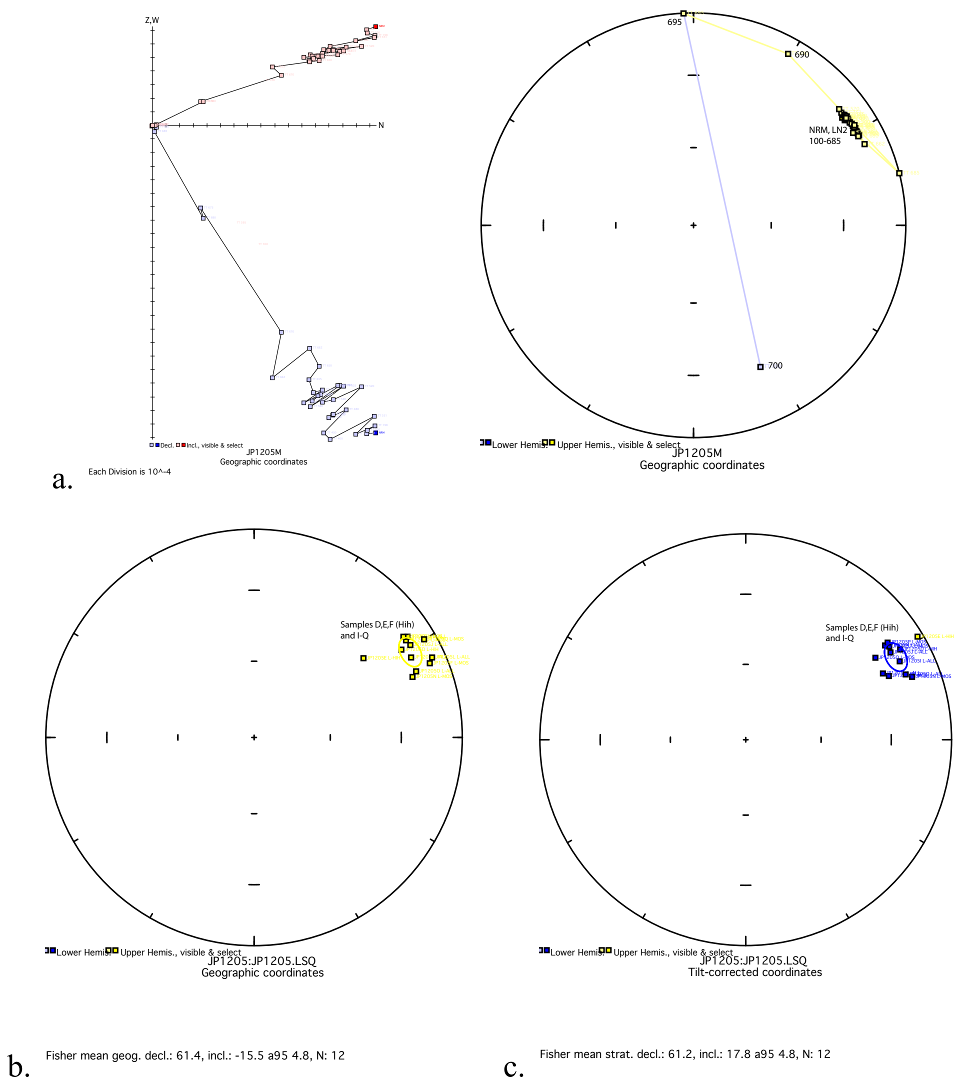

Figure 17. (a) Representative [LEFT] Zijderveld diagrams and [RIGHT] equal area plots for sample M JP1205 with (b) geographic mean and (c) tilt-corrected mean for samples D-F (high temperature component), I-Q.

Site JP1207 is sampled from the western contact of dyke JP1206, which is of mafic composition. The dyke is located about 50 m east of dyke JP1204 and contains calcite veins varying in size from 1 mm to 2 cm. Similar to dykes JP1102 and JP1204, dyke JP1206 has a north and up direction of 017.4°, -30.4° (Fig. 18).

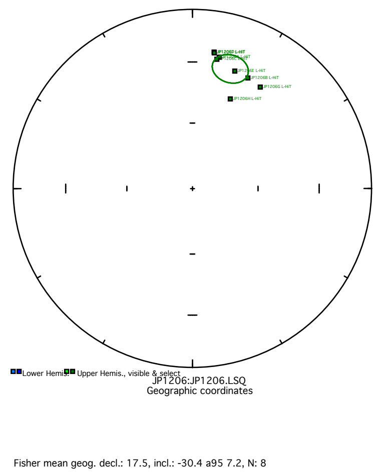

Figure 18. Mean magnetic direction for mafic dyke JP1206.

Samples A and B of site JP1207 both have a single component, with steady demagnetization until 575°C, where there is a jump to the origin, indicating magnetite was likely present (Fig. 19a). These two samples have similar direction to dyke 1206 (north and up). Samples C-F had two components, the low temperature components also being north and shallow (Fig. 19b). The geographic mean from these samples gives a declination of 020.2° and an inclination of -18.3° and an A_{95} of 12.5°, agreeing with the magnetization direction of dyke JP1206.

Sample G in JP1207, shown in Figure 20a, is a hybrid between the observed dyke direction of north and shallow and the assumed Barby direction of northeast and shallow. Most of the demagnetization occurs from 685°C to 690°C, which is a strong indication of hematite. Samples H-L also lose most of their magnetization at 685°C, and almost all have a single component that is northeast and shallow (Fig. 20b). Using the high temperature components from samples C-F, as well as samples H-L a geographic mean for the Barby was calculated to be 065.0°, -20.5° and tilt-corrected was 065.5°, 13.8°, with an A_{95} value of 3.3 (Fig. 20c,d).

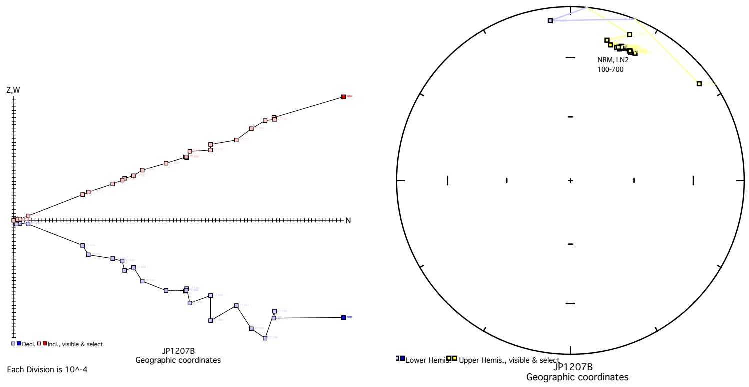

a.

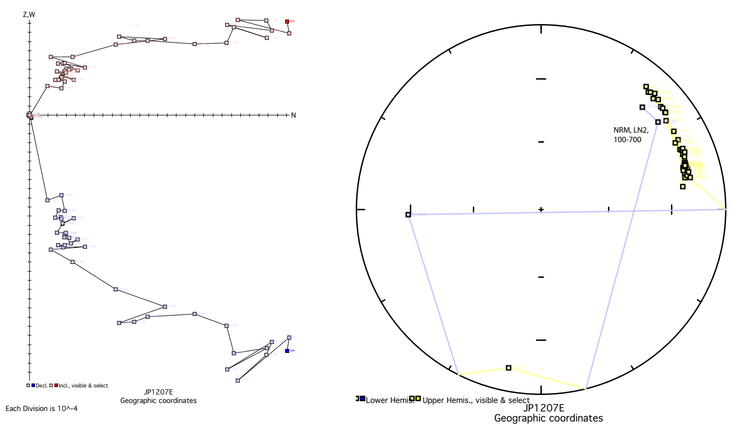

b.

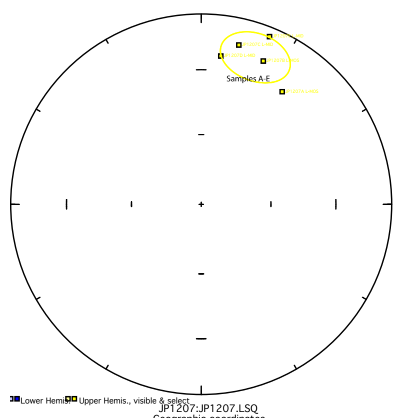

c. Fisher mean geog. decl.: 20.2, incl.: -18.3 a95 12.5, N: 5

Figure 19. Representative [LEFT] Zijderveld diagrams and [RIGHT] equal area plots for samples (a) B and (b) E in JP1207 with the (c) mean geographic direction for samples A-E

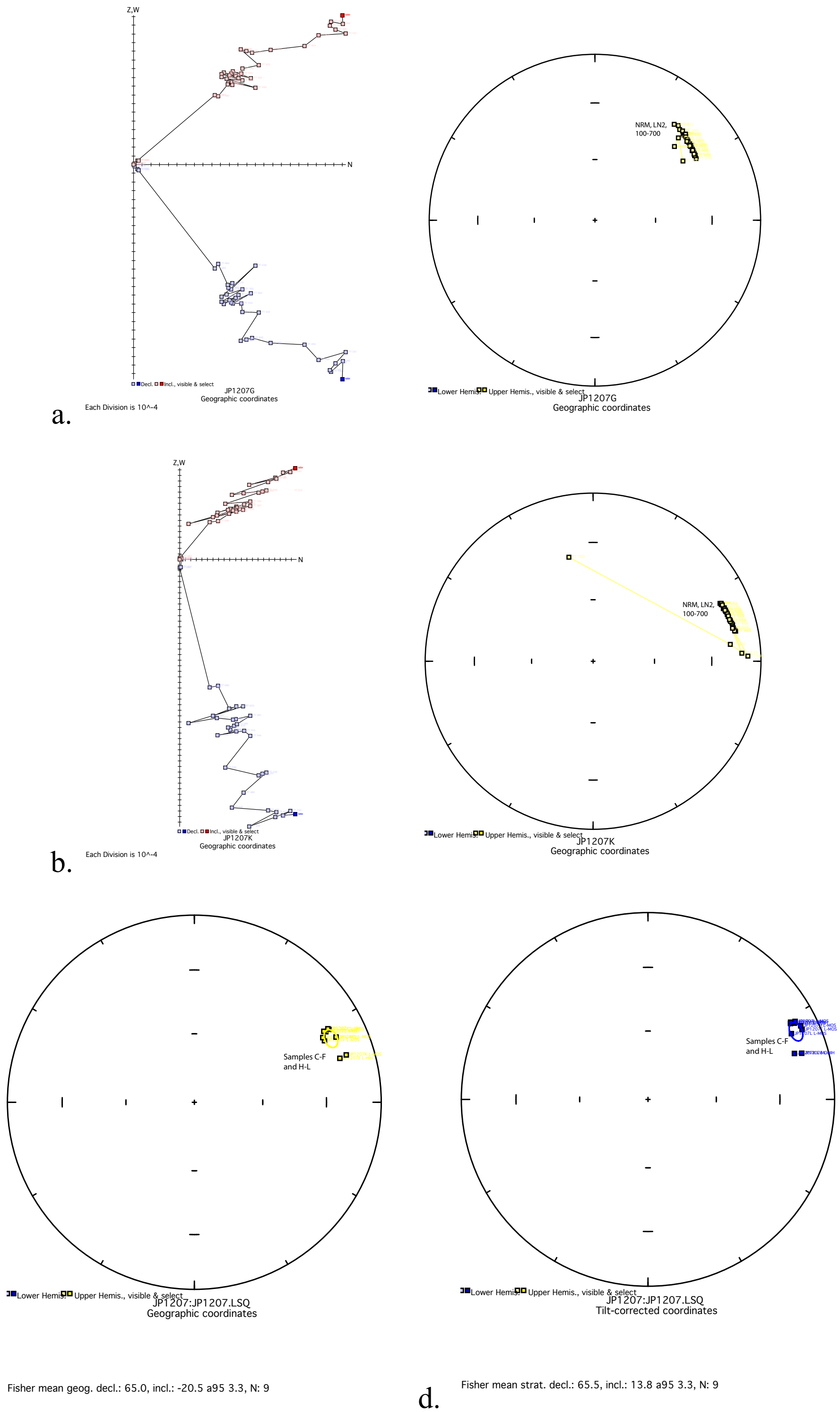

Figure 20. Representative [LEFT] Zijderveld diagrams and [RIGHT] equal area plots for samples (a) G and (b) K in JP1207 with the (c) geographic and (d) tilt-corrected means for samples C-F,H-L.

All three sites in this locality resulted in a positive BCT, with the lavas closest to the intruding dykes showing the influence of the dyke's magnetization (north and shallow) while the host Barby lavas further away from the contacts of the dykes consistently resulted in a northeast and shallow direction.

3.3. Central locality JP1208

Site JP1208 was sampled from the western edge of dykes JP1103 and JP1104 (Fig. 21). This was a rhyolitic dyke that had a mafic rim of 1-2 m on either side. The BCT starts at the contact with JP1104, with the sampled Barby occurring in a well-exposed streambed. The lavas are highly fractured near the contact, become more coherent towards the stream, and have some epidote alteration. The Barby lavas outcrop again amongst the sand in the streambed, which include some mafic components. This area was sampled but is possibly not in situ. Additionally, there appeared to be a rhyolitic dyke that was poorly exposed to the north of JP1208, but no contact could be seen.

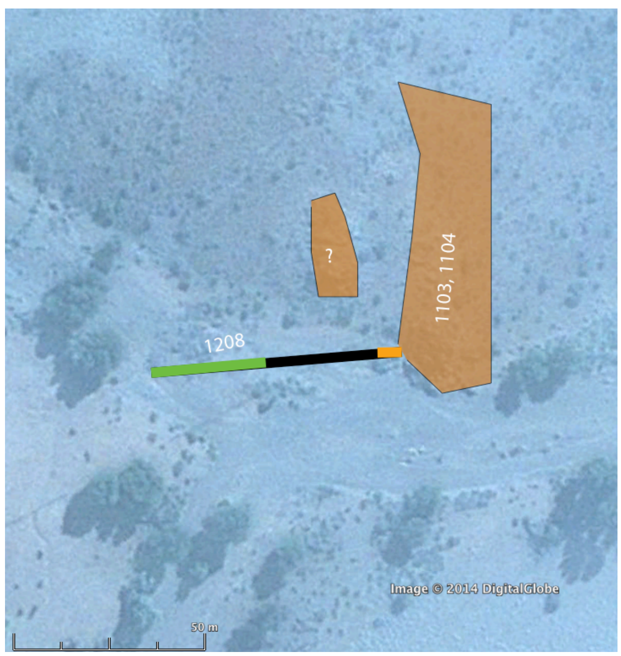

Figure 21. Schematic of the relation between sampled barby Fm. at site JP1208 and nearby sampled dykes at JP1103 and JP1104. Possible dyke exposure to the north of JP1208 samples. In JP1208, orange denotes a possible dyke direction and green denotes a possible host rock direction.

The dykes sampled here at JP1103 and JP1104 have no coherent magnetic direction and appear to have been lightning struck. Although a BCT could not be conclusively preformed due to the lack of data from the dykes, JP1208 was still analyzed so that it could be compared to the western and eastern localities. Samples A-K all have a single magnetic component that is north and up (Fig. 22a). These samples give a geographic mean direction of 003°, -48.6° and an A_{95} of 5.1° (Fig. 22b), which could possibly be interpreted as the dyke's magnetization, since this direction is consistent with other dykes in the area.

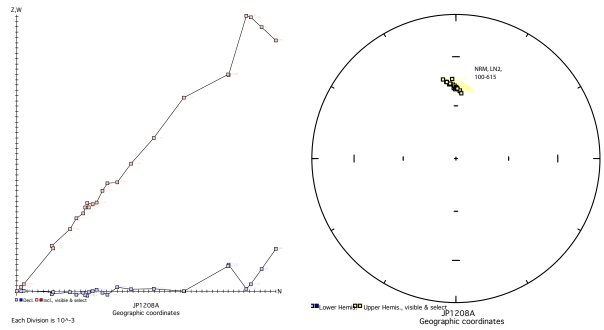

a.

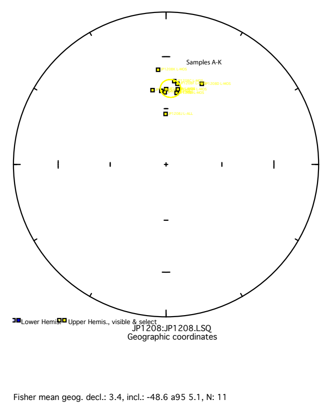

b.

Figure 22. JP1208 a. Sample A near contact b. Geographic mean direction from samples A-K.

One can strongly suspect the samples closest to the intrusion are recording the remagnetization from the intruding dyke and can be inferred from samples A-K that it might have been north and up. Though sample L is possibly a hybrid, samples M-S all had varying components and directions. It should be noted that this area contained possible lavas that were not in situ, as well as some mafic sections. Sample S is from a mafic exposure and is shown in Figure 23a. Samples T-Z all had their high or single component displaying a north and down direction, with most of the demagnetization occurring at 560°C (Fig. 23b). The resulting geographic Fisher mean from samples T-Z is 010.6°, 23.0°, tilt-corrected to 351.9°, 33.4° with an A_{95} of 7.1° (Fig. 23c,d). The results of samples T-Z provide a magnetic direction for the Barby that is different than previously observed It is possible that the NE and up sites were locally rotated. It remains to be seen what the true Barby direction is for the region. The different magnetic directions could both be Barby but of very different ages, perhaps due to a drift of the polar craton. Unfortunately, this test is unclear and cannot be considered a full baked contact test.

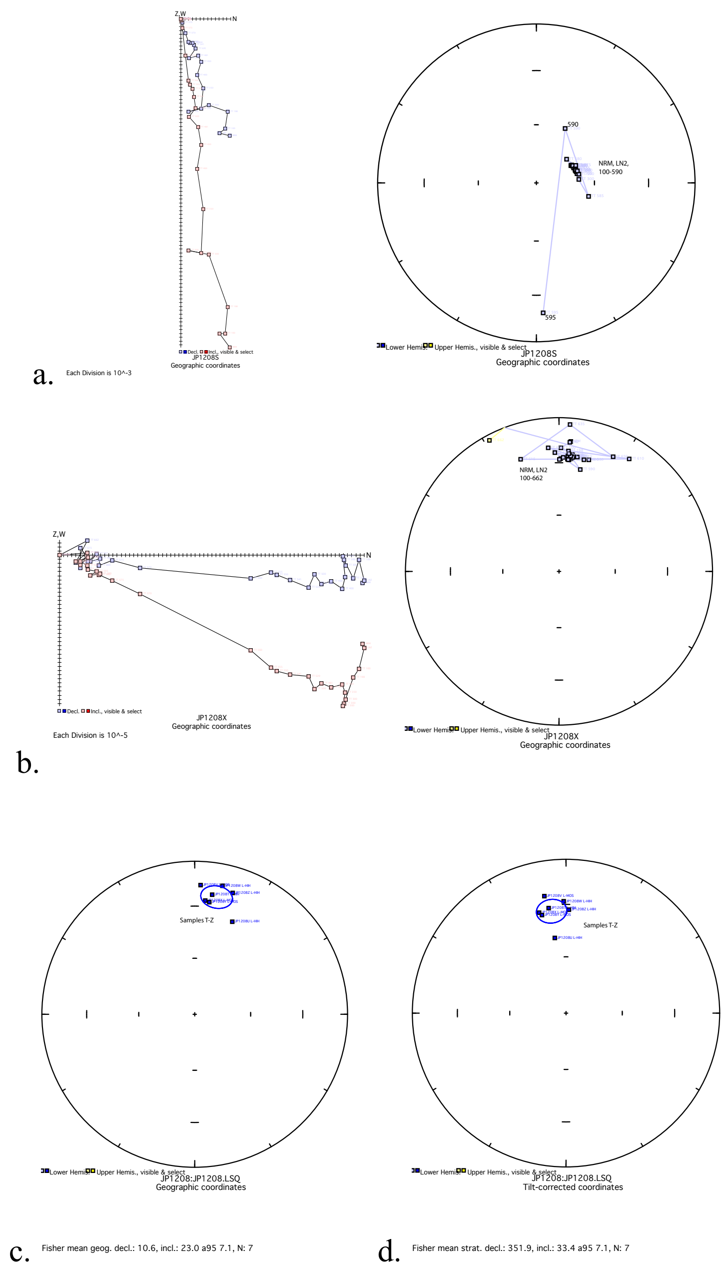

Figure 23. JP1208 a. Sample S in mafic zone b. Sample X away from contact c. Geographic mean direction from samples T-Z d. Tilt-corrected mean direction from samples T-Z.

3.4 Eastern localities JP1218, 1219, 1220

Sites JP1218, 1219, and 1220 were all sampled very near the Guperas angular unconformity with rhyolitic dyke JP1219 (12 m wide) intruding both the Barby and the overlying Guperas (Fig. 24). The dyke has a trend of 044°, 78° at the northern margin, with a noticeable chill margin in the rhyolite.

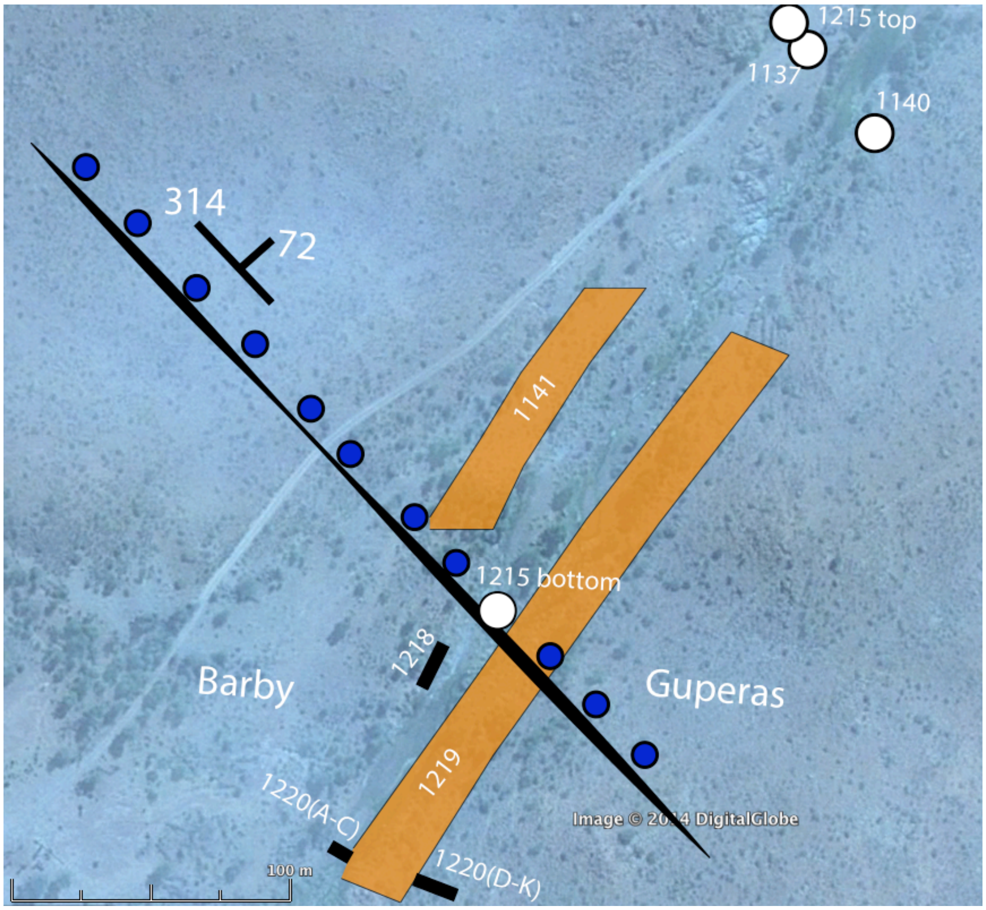

Figure 24. Barby sites JP1218 and JP 1220. Intruding dykes JP1219 and JP1141. Angular unconformity between Barby Fm. and Guperas Fm. denoted by black line with blue circles.

Dyke JP1219 did not display a single magnetic direction, but rather demagnetized from a north and shallow direction, until it reached a stable endpoint (SEP) of a southeast and shallow direction (Fig. 25). The lower temperature components are north and shallow and gave a mean of 022.1°, 13.6° with an A_{95} of 13.3. The SEP of the samples is southeast and gave a mean of 157.6°, -31.2°, with a corresponding A_{95} of 10.6.

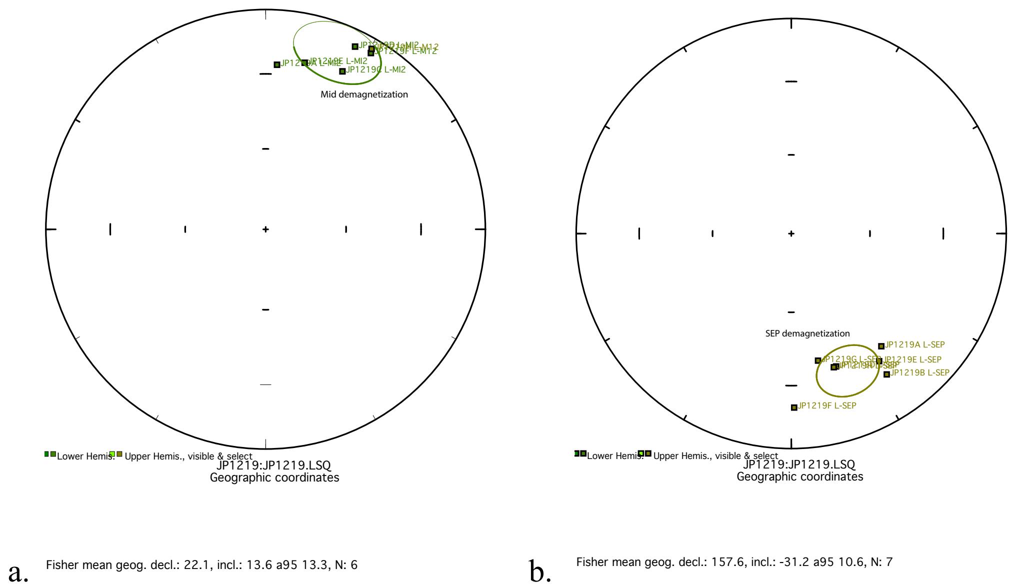

Figure 25. Mean magnetic directions for dyke JP1219 (a) from the middle temperature demagnetization and (b) from the stable endpoint (SEP) demagnetization

JP1218 was sampled approximately 10m away from the Barby-Guperas contact. Of the 8 samples taken at 1218, 6 were used, as samples A and B appear to be affected by lightning strikes. Almost all of the remaining 6 had a single component that gave a north and shallow direction (Fig. 26a). This resulted in a geographic declination of 006.8° and inclination of 18.1°, with an A_{95} value of 5.0° (Fig. 26b), which was similar to that observed in the lower and middle temperatures of dyke JP1219. The bedding in the Barby Formation was not evident at this locality, so the bedding was tilt-corrected for the dip of the overlying Guperas strata (314° strike, 72° dip). The Guperas was restored to horizontal, restoring the Barby pole bedding to 086° trend, 21° plunge, which is used to calculate the tilt correction giving a new declination of 356.7° and an inclination of -38.6°.

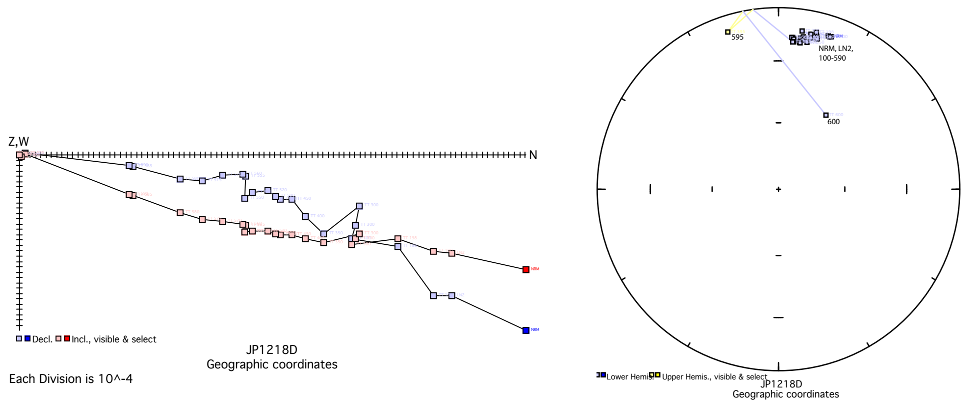

a.

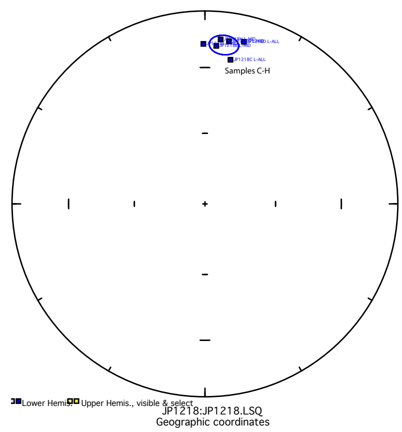

b. Fisher mean geog. decl.: 6.8, incl.: 18.1 a95 5.0, N: 6

Figure 26. JP1218 with (a) sample D and (b) geographic mean direction from samples C-H.

Site JP1220 was sampled to either side of the JP1219 dyke, with samples A-C less than 1 m away from the contact on the western edge, and samples D-K taken on the eastern edge ranging from less than 1 m to 4 m from the dyke. Besides sample I, which was lightning struck, nearly every sample has a middle temperature component (~400°C-570°C) and a high temperature component (~570°C-600°C) as seen in Figure 27a. Two means were computed for this site, one with the middle temperatures and one with the high temperatures. The high temperature geographic mean is 002.7°, 16.2°, tilt-corrected to 350.5°, 21.2° with an A_{95} of 10.0 (Fig. 27b). The mean from the middle temperatures is 160.8°, -03.9°, tilt-corrected to 160.0°, 01.3°, with an A_{95} value of 25.2 (Fig. 27c). The high and middle temperature directions are the reverse of those seen in dyke JP1219, as its high component was southeast and shallow, while its lower temperature component displayed the north and shallow direction.

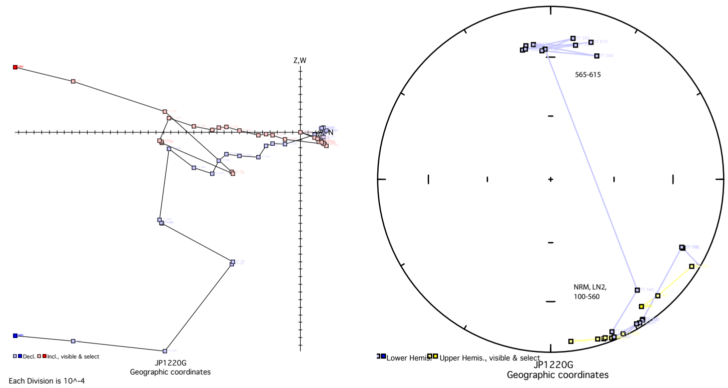

a.

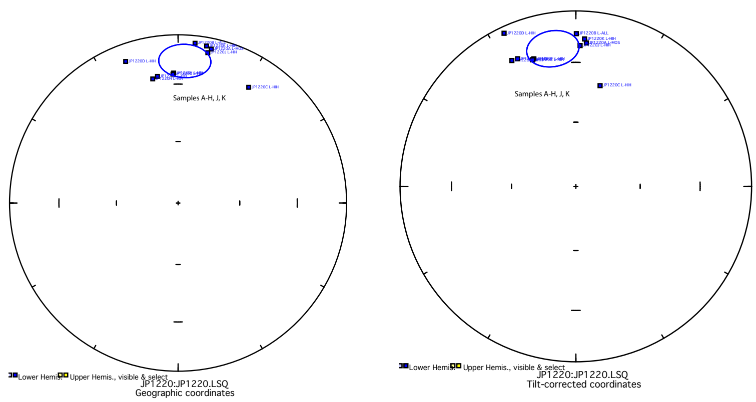

b. Fisher mean geog. decl.: 2.7, incl.: 16.2 a95 10.0, N: 10

Fisher mean strat. decl.: 350.5, incl.: 21.2 a95 10.1, N: 10

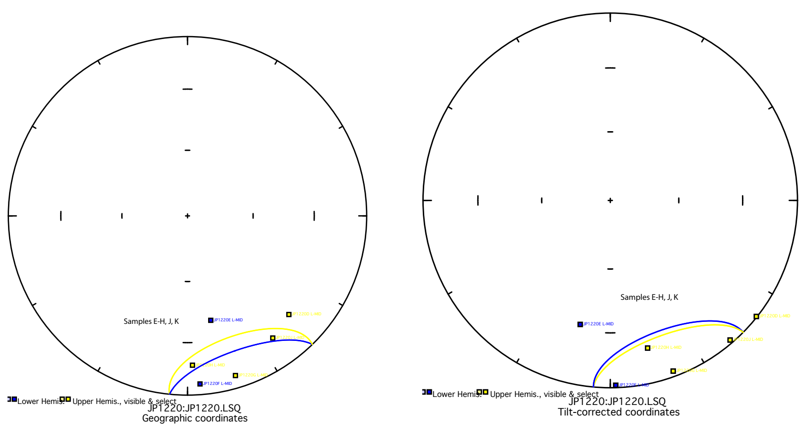

c. Fisher mean geog. decl.: 160.8, incl.: -3.9 a95 25.2, N: 6

Fisher mean strat. decl.: 160.0, incl.: 1.3 a95 25.2, N: 6

Figure 27. Results for JP1220 a. Sample G b. samples A-H, J, K in [LEFT] geographic and [RIGHT] tilt-corrected coordinates c. samples E-H, J, and K in [LEFT] geographic and [RIGHT] tilt-corrected coordinates.

4. DISCUSSION

4.1 Western localities

Site JP1202 was sampled next to rhyolitic dyke JP1101, which potentially had magma that intruded at low temperatures and appears to be highly oxidized that could contain both magnetite and hematite. The hematite in the host rock could cause a narrow baked zone. Using all 8 samples from JP1202, the remanent direction for the Barby site was northeast and shallow. This direction is significantly different than the JP1101 dyke direction, which was south and shallow. Together, sites JP1101 and site JP1202 confirm a positive baked-contact test for the dyke, indicating that the magnetization of the post-Guperas dykes is primary. In addition, this implies that the shallow northeast remanence direction of the Barby formation is older than the age of dyke intrusion.

Since site JP1203 is between dykes sampled at JP1102 and JP1204, the results are slightly more complex, but still yield a positive BCT. Samples A-G show a north and shallow magnetization direction that corresponds with that of the dyke sampled at JP1102. Samples H, I, and J retained the Barby direction of northeast and shallow. The end of section JP1203 was located south of dyke JP1204 and appears to show some influence of that dyke's magnetization. Samples K and O both have a direction that agrees with the north and shallow direction of dyke JP1204, suggesting that the intruding dyke may have remagnetized them.

Site JP1205 was a BCT with dyke JP1204 from its eastern contact with 13 out of the 17 samples were used in analysis (B, G, and H had unclear results). JP1205 has a clear transition from dyke to Barby direction. Samples A and C have been remagnetized by dyke JP1206 and show a direction of north and shallow. Samples D and E have low components of dyke direction and high components that are northeast and shallow – the Barby direction. Samples F to Q also have the Barby direction northeast and shallow further supporting this positive BCT result.

Site JP1207 also had a positive BCT with dyke JP1206. Samples A and B have the dyke's direction. Samples C-F of JP1207 have both low temperature and high temperature components. The low temperature component corresponds with the dyke direction, and the high temperature component being the Barby direction. Sample G has a mild inflection, but both components were clearly in between the two modes and appear to have substantial overlap. The overlapping, interlocking spectra of the two components contaminate each individual magnetic direction on G. Samples H-L primarily exhibit Barby magnetic direction, with some small inflection at low temperatures.

The magnetic evidence from the western localities suggests that the Barby Formation retained its magnetization prior to the intrusion of the post-Guperas dykes in that area. The positive BCTs from sites JP1202, JP1203, JP1205, and JP1207 imply the magnetization of the Barby lavas predates that of the Guperas lavas, after folding events. This would mean that if there was any remagnetization, it must have occurred before folding and would have localized effects, not widespread. This chronology of events is in agreement with Piper's 1975 results.

4.2 Central and Eastern localities

Nothing conclusive can be determined from site JP1208. The JP1103 dyke direction was scattered, most likely due to lightning strike, making a BCT at this site impossible to do. Samples farther away from the dyke show a north and up direction. This could be a primary Barby direction or an overprint. There are some unusual and irregular directions from samples L-T. Within that interval, there are several jumps back to both the dyke direction and the host's direction. One possibility is that there were multiple lightning strikes in these locations. There are rhyolite exposure north of mafic samples R and S, but no contact could be found, perhaps implying these exposures are not in situ. It is possible that a pinching of a rhyolitic dyke to the north, that potentially had a mafic rim, could have remagnetized some of these middle samples. However, not enough samples were collected close to the possible contact zone, if there even is one present, so this can be neither confirmed nor dismissed. The overall lack of exposure in sample zone prevents us from understanding this. Regardless, the northern rhyolitic exposure appears to have some influence on the magnetic direction of the sampling site.

Site JP1218 was taken near a 14 m wide dyke (JP1219) that could have influenced the surrounding area, overprinting the Barby direction. There is the slight possibility that JP1218 gives a Barby direction that is similar to the Barby at site JP1208, and the adjacent dyke happens to have a similar direction as the Barby that would be due either to secular variation or minimal drift between the two time periods.

Site JP1220 has a curious relationship to the JP1219 dyke, as that dyke has low/mid temperature components of north and down and its stable end point (SEP) is southeast and up. The dyke could have then influence the surrounding Barby given that the SEP of the dyke is similar to the low/mid temperature steps of the Barby from JP1220. This is possibly due to a local hydrothermal alteration that shows up as hematite in JP1219 as well as the low thermal steps of JP1220. The high temperature components are most likely influenced by the dyke, as many of the samples are less than 1 meter from the both the western and eastern contacts.

The overlaying Guperas data has a scattered direction of mostly north and down from the JP1215 sampled stratigraphic section. At the time the Guperas was flat, the Barby was dipping ~70° to the west (angle between the Guperas and the Barby). Sites JP1208, 1218, and 1220 all show the same direction as the overlying Guperas section (Panzik et al., in prep) of north and up. Likely, the Barby Fm. and the Guperas stratigraphic sequence have been overprinted by the nearby intruding dykes, and thus implies the magnetization of the Barby from these sites is not primary.

4.3 Virtual geomagnetic poles

Three mean poles were calculated from the presented data. From the central and western localities, the north and down mean direction is 53.8°N, 027.9°E and the less prevalent southeast and down mean direction is 49.5°N, 027.9°E. The mean geographic Barby direction of northeast and shallow is 33.5°N, 099.7°E and tilt-corrected is 25.5°N, 085.2°E. These calculated means are plotted on the polar wander path from Gose et al. (2013) in Figure 28.

The southeast up and north down directions fit the path of the craton and appear to be ~1100 Ma. The more prevalent north and down direction is very similar to Piper's results for the Barby. This suggests that Piper's Barby direction is not the primary magnetization, but is an overprint direction that occurred post-Guperas. The new calculated Barby direction is further to the northeast than previously thought. Because of the small sample size, the uncertainty of the mean is on the order of 25-35°. This is reasonable, as it is near the Kimberlite mean, as well as being younger than the post-Guperas dykes that have been dated at ~1105 Ma. Additionally, the mean pole direction appears to have an age older than 1200

Ma, in agreement with the correlated lavas to the west (Hoal and Heaman, 1995) that were dated to be 1215-1220 Ma using U-Pb age constraints on the Awasib Mountains.

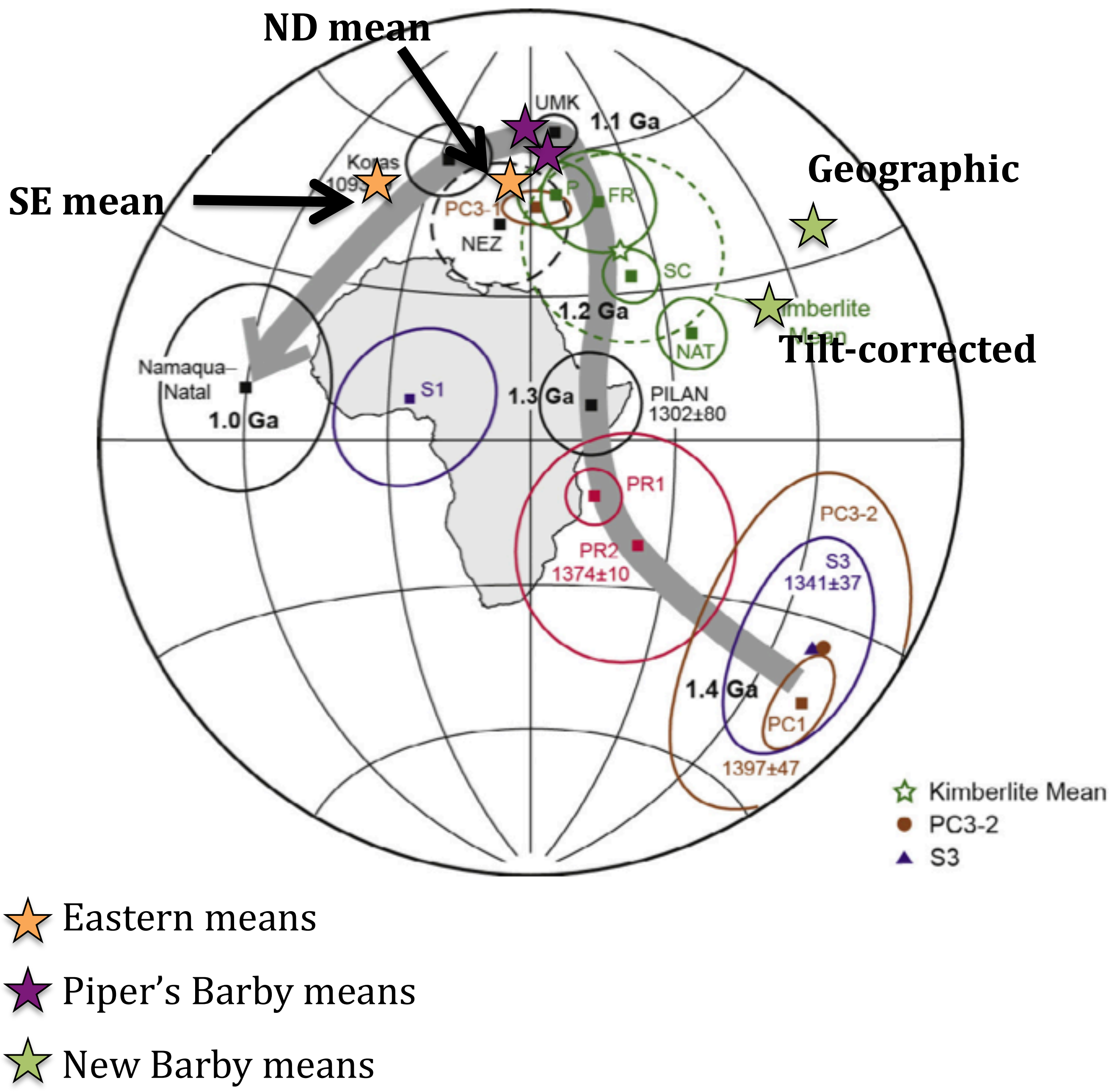

Figure 28. Kalahari apparent polar wander path (APW) with calculated means. Modified from Gose et al. (2013). SE = southeast mean from sites 1219 and 1220. ND = north and down mean from sites 1218, 1219, and 1220. Geographic and Tilt-corrected Barby means calculated from sites 1202, 1203, 1205, and 1207.

5. CONCLUSION

In Piper's study, the Barby Formation was sampled further to the south of our field locality and had results with much stronger remanent magnetizations than the samples in this study that were further to the north. The strong magnetizations could suggest magnetic overprinting that supports the results of this study, and again implies that the Barby magnetization determined by Piper was not primary. The direction of the Barby Formation from site JP1202 agrees with the host rocks from sites JP1203, 1205, and 1207, supporting the new apparent polar wander path of being northeast and shallow and challenging Piper's result of a north and shallow direction. The complicated nature of the central and eastern localities suggests they were remagnetized by nearby dyke intrusions or large deformations. Most likely, they have been overprinted since the deposition of the Guperas Formation. Even given the small sample size, the new Barby poles calculated in this study strongly suggest a northeast and shallow direction. The promising results of this initial study invite further work to be done on the Barby Formation.

ACKNOWLEDGEMENTS

Dave Evans, Joe Panzik, Yale University Geology & Geophysics Department, Jennifer Kasbohm, Paul Hoffman, Charlie Hoffmann, the Miller family

REFERENCES

Butler, Robert F., 1998. Paleomagnetism: Magnetic Domains to Geologic Terranes. University of Arizona, Tucson, Arizona. 99-100.

Buchan, K. 2007. Baked Contact Test*, Encyclopedia of Geomagnetism and Paleomagnetism.* 35-39.

Beetz, P. F. W., 1923. The Konkip Formation on the border of the Namib Desert north of Aus, *Trans. Geol. Soc. S. Afr*. 25, 23-40.

Everitt, C. W. F. and Clegg, J. A., 1962. A Field Test of Palaeomagnetic Stability. *Geophys J Roy Astr S*, 312-319.

Fisher, R., 1953. Dispersion on a sphere. *Proceedings of the Royal Society of London. Series A,* 217, 295-305.

Gubbins, David, and Herrero-Bervera, Emilio ed., 2007. Encyclopedia of Geomagnetism and Paleomagnetism. Springer, The Netherlands, 35-38.

Hanson, R.E., Crowley, J.L., Bowring, S.A., Ramezani, J., Gose, W.A., Dalziel, I.W.D., Pancake, J.A., Seidel, E.K., Blenkinsop, T.G. & Mukwakwami, J., 2004. Coeval 1.1 billion year old large-scale magmatism in the Kalahari and Laurentian cratons during Rodinia supercontinent assembly. *Science,* 304, 1126–1129.

Hoal, B.G. and Heaman, L.M. 1995. The Sinclair Sequence: U-Pb age constraints from the Awasib Mountain area. Communication of the Geologic Survey of Namibia 10. 83-91.

Kasbohm, J. et al., Paleomagnetic and geochronologic data from Late Mesoproterozoic redbed sedimentary rocks on the western margin of the Kalahari craton. *GSL,* submitted.

Kirschvink, J.L., 1980. The least-squares line and plane and the analysis of palaeomagnetic data. *Geophys. J. Intl.*, 62, 699-718.

Kirschvink, J.L., Kopp, R.E., Raub, T.D., Baumgartner, C.T., and Holt, J.W., 2008. Rapid, precise, and high-sensitivity acquisition of paleomagnetic and rock-magnetic data: Development of a low-noise automatic sample-changing system for superconducting rock magnetometers. Geochemistry, Geophysics, Geosystems, 9(5), Q05Y01, doi:10.1029/2007GC001856.

Kröner, A. and Rankama, K., 1972. Late Precambrian glaciogenic sedimentary rocks in southern Africa: A compilation with definitions and correlations, Bull. No. 11, Precambrian Research Unit, University of Cape Town, 37.

Martin, H., 1965. Precambrian geology of South west Africa and Namaqualand, Precambrian Research Unit, University of Cape Town, 159.

Miller, R.McG., 2008. Chapter 8: The Sinclair Supergroup. In: Miller, R.McG., The Geology of Namibia Volume 1: Archaean to Mesoproterozoic. *Ministry of Mines and Energy, Geological Survey of Namibia*, pp. 8-1 to 8-67.

Panzik, J. et al., Using Paleomagnetism and geochronology data to determine paleogeographic and tectonic relations of the Sinclair Terrane, Namibia, *in prep.*

Thomas, R.J., Agenbacht, A.L.D., Cornell, D.H. & Moore, J.M., 1994. The Late Kibaran of southern Africa: Tectonic evolution and metallogeny. *Ore Geology Reviews* 9, 131-160.

von Brunn, V., 1969. Igneous rocks of the Nagatis and Sinclair Formations Northeast of Luderitz, South West Africa, Bull. No. 7, Precambrian Research Unit, University of Cape Town, 54.

Watters, B.R., 1977. The Sinclair Group: Definition and regional correlations. *Transactions of the Geological Society of South Africa* 80, 9-16.

Sample	ID	NRM	LN2	100	198	300	351	400	450	480	500	520	540	550	555	560	565	570	575	580	585	590	595	615	635	650	662	670	675	680	685	690	695	700	origin	Geographic Declination	Geographic Inclanation	MAD
A	all	x	x	x	x	x	x	x	x	x	x	x	x	x	x	x	x	x	x	x	x	x	x	x	x	x	x	x	x	x	x	x	x	x	x	055	-15	3.1
B	all	x	x	x	x	x	x	x	x	x	x	x	x	x	x	x	x	x	x	x	x	x	x	x	x	x	x	x	x	x	x	x	x	x	x	048	-26	2.6
C	all	x	x	x	x	x	x	x	x	x	x	x	x	x	x	x	x	x	x	x	x	x	x	x	x	x	x	x	x	x	x	x	x	x	x	053	-17	3.3
D	all	x	x	x	x	x	x	x	x	x	x	x	x	x	x	x	x	x	x	x	x	x	x	x	x	x	x	x	x	x	x	x	x	x	x	044	-23	2.8
E	all	x	x	x	x	x	x	x	x	x	x	x	x	x	x	x	x	x	x	x	x	x	x	x	x	x	x	x	x	x	x	x	x	x	x	045	-10	2.6
F	mos				x	x	x	x	x	x	x	x	x	x	x	x	x	x	x	x	x	x	x	x	x	x	x	x	x	x	x	x	x	x	x	050	-15	2.1
G	mos				x	x	x	x	x	x	x	x	x	x	x	x	x	x	x	x	x	x	x	x	x	x	x	x	x	x	x	x	x	x	x	055	01	2.8
H	mos							x	x	x	x	x	x	x	x	x	x	x	x	x	x	x	x	x	x	x	x	x	x	x	x	x	x	x	x	055	-32	2.9

Sample	ID	NRM	LN2	100	198	300	351	400	450	480	500	520	540	550	555	560	565	570	575	580	585	590	595	615	635	650	662	670	675	680	685	690	695	700	Origin	Geographic Declination	Geographic Inclanation	MAD
A	mos					x	x	x	x	x	x	x	x	x	x	x	x	x	x	x	x	x	x	x	x	x	x	x	x	x	x	x	x	x	x	015	-45	1.2
B	mos						x	x	x	x	x	x	x	x	x	x	x	x	x	x	x	x	x	x	x	x	x	x	x	x	x	x	x	x	x	019	-46	1.4
C	mos					x	x	x	x	x	x	x	x	x	x	x	x	x	x	x	x	x	x	x	x	x	x	x	x	x	x	x	x	x	x	020	-46	2.4
D	all	x	x	x	x	x	x	x	x	x	x	x	x	x	x	x	x	x	x	x	x	x	x	x	x	x	x	x	x	x	x	x	x	x	x	012	-44	1.3
E	all	x	x	x	x	x	x	x	x	x	x	x	x	x	x	x	x	x	x	x	x	x	x												x	032	-58	3.0
F	low	x	x	x	x	x	x	x	x	x																										230	49	5.7
	hih									x	x	x	x	x	x	x	x	x	x	x	x	x	x												x	016	-43	2.3
G	all	x	x	x	x	x	x	x	x	x	x	x	x	x	x	x	x	x	x	x	x	x	x												x	027	-39	2.5
H	low	x	x	x	x	x	x	x	x	x	x	x																								017	-27	15.6
	mid											x	x	x	x	x																				016	-41	6.4
	hih															x	x	x	x	x	x	x	x	x	x	x	x	x	x	x	x	x	x	x	x	054	-12	5.0
I	low	x	x	x	x	x	x	x	x	x																										001	-47	10.7
	mid									x	x	x	x	x	x	x																				037	-41	7.3
	hih															x	x	x	x	x	x	x	x	x	x	x	x	x	x	x	x	x	x	x	x	061	-02	4.3
J	mid							x	x	x	x	x	x	x	x	x	x	x																		051	-41	5.3
	hih																	x	x	x	x	x	x	x	x	x	x	x	x	x	x	x	x	x	x	073	-07	4.8
K	low	x	x	x	x	x	x	x																											x	246	-21	6.2
	mid							x	x	x	x	x	x	x	x	x	x																			339	-49	12.9
	hih																x	x	x	x	x	x	x	x	x	x	x	x	x	x					x	015	-48	2.2
L	all	x	x	x	x	x	x	x	x	x	x	x	x	x	x	x	x	x	x	x	x	x	x												x	181	33	2.1
M	all	x	x	x	x	x	x	x	x	x	x	x	x	x	x	x	x	x	x	x	x	x	x												x	182	42	1.2
N	low		x	x	x	x	x	x	x																											255	66	6.2
	mid								x	x	x	x	x	x	x	x																				332	22	13.8
	hih															x	x	x	x	x	x	x	x												x	004	-37	3.3
O	low					x	x	x	x	x	x	x																								018	-31	8.2
	mid											x	x	x	x	x	x	x	x	x	x	x	x													011	51	9.6
	hih																						x	x	x	x	x	x	x	x	x				x	154	43	9.0
	sep																						x	x	x	x	x								x	152	43	5.0

Sample	ID	NRM	LN2	100	198	300	351	400	450	480	500	520	540	550	555	560	565	570	575	580	585	590	595	615	635	650	662	670	675	680	685	690	695	700	Origin	Geographic Declination	Geographic Inclanation	MAD
A	low	x	x		x			x	x	x	x	x																								058	-50	9.4
	hih											x	x	x	x	x	x	x	x	x	x	x	x												x	026	-38	3.1
B	mos		x	x	x	x	x	x	x	x	x	x	x	x	x	x	x	x	x	x	x	x	x												x	041	23	5.7
C	mos				x	x	x	x	x	x	x	x	x	x	x	x	x	x	x	x	x	x	x												x	014	-43	1.9
D	mid						x	x	x	x	x	x	x	x																						012	-35	4.8
	hih													x	x	x	x	x	x	x	x	x	x	x	x	x	x	x	x	x					x	059	-19	5.4
E	mos	x	x	x	x	x	x	x	x	x	x	x	x		x	x	x	x	x	x	x	x	x	x	x	x	x	x	x	x	x	x	x	x	x	045	-39	5.6
	mid						x	x	x	x	x	x	x	x																						023	-44	12.6
	hih													x	x	x	x	x	x	x	x	x	x	x	x	x	x	x	x	x	x	x	x	x	x	054	-35	4.4
F	mid				x	x	x	x	x	x																										011	-38	6.7
	mos									x	x	x	x	x	x	x	x	x	x	x	x	x	x	x	x	x	x	x	x	x	x	x	x	x	x	067	-09	2.5
G	mos								x	x	x	x	x	x	x	x	x	x	x	x	x	x	x	x	x	x	x								x	345	-38	3.8
H	n/a																																					
I	all	x	x	x	x	x	x	x	x	x	x	x	x	x	x	x	x	x	x	x	x	x	x	x	x	x	x	x	x	x	x	x	x	x	x	063	-17	2.7
J	all	x	x	x	x	x	x	x	x	x	x	x	x	x	x	x	x	x	x	x	x	x	x	x	x	x	x	x	x	x	x	x	x	x	x	059	-14	3.2
K	mos								x	x	x	x	x	x	x	x	x	x	x	x	x	x	x	x	x	x	x	x	x	x	x	x	x	x	x	057	-15	2.0
L	all	x	x	x	x	x	x	x	x	x	x	x	x	x	x	x	x	x	x	x	x	x	x	x	x	x	x	x	x	x	x	x	x	x	x	066	-07	3.6
M	all	x	x	x	x	x	x	x	x	x	x	x	x	x	x	x	x	x	x	x	x	x	x	x	x	x	x	x	x	x	x	x	x	x	x	057	-13	2.8
N	mos		x	x	x	x	x	x	x	x	x	x	x	x	x	x	x	x	x	x	x	x	x	x	x	x	x	x	x	x	x	x	x	x	x	069	-20	4.3
O	all	x	x	x	x	x	x	x	x	x	x	x	x	x	x	x	x	x	x	x	x	x	x	x	x	x	x	x	x	x	x	x	x	x	x	068	-17	4.0
P	mos						x	x	x	x	x	x	x	x	x	x	x	x	x	x	x	x	x	x	x	x	x	x	x	x	x	x	x	x	x	056	-15	3.8
Q	mos					x	x	x	x	x	x	x	x	x	x	x	x	x	x	x	x	x	x	x	x	x	x	x	x	x	x	x	x	x	x	060	-06	4.5

Sample	ID	NRM	LN2	100	198	300	351	400	450	480	500	520	540	550	555	560	565	570	575	580	585	590	595	615	635	650	662	670	675	680	685	690	695	700	Origin	Geographic Declination	Geographic Inclanation	MAD
A	mos						x	x	x	x	x	x	x	x	x	x	x	x	x	x	x	x	x	x	x	x	x	x	x	x	x	x	x	x	x	036	-28	3.8
B	mos				x	x	x	x	x	x	x	x	x	x	x	x	x	x	x	x	x	x	x	x	x	x	x	x	x	x	x	x	x	x	x	023	-19	2.0
C	mid							x	x	x	x	x	x	x	x																					013	-15	9.6
	mos												x	x	x	x	x	x	x	x	x	x	x	x	x	x	x	x	x	x	x	x	x	x	x	062	-19	3.5
D	low							x	x	x	x	x																								022	-30	5.8
	mid							x	x	x	x	x	x	x																						008	-23	8.8
	hih														x	x	x	x	x	x	x	x	x	x	x	x	x	x	x	x	x	x	x	x	x	062	-21	5.3
E	low				x	x	x	x	x	x	x	x	x	x	x	x	x	x	x	x	x															024	-07	7.2
	mid							x	x	x	x	x	x																							022	-06	15.1
	hih												x	x	x	x	x	x	x	x	x	x	x	x	x	x	x	x	x	x	x	x	x	x	x	073	-20	3.5
F	mos	x	x	x	x	x	x	x	x	x	x	x	x	x	x	x	x	x	x	x	x	x	x	x	x	x	x	x	x	x	x	x	x	x	x	065	-24	2.8
G	all	x	x	x	x	x	x	x	x	x	x	x	x	x	x	x	x	x	x	x	x	x	x	x	x	x	x	x	x	x	x	x	x	x	x	049	-27	4.2
H	mos									x	x	x	x	x	x	x	x	x	x	x	x	x	x	x	x	x	x	x	x	x	x	x	x	x	x	063	-24	2.2
I	mos								x	x	x	x	x	x	x	x	x	x	x	x	x	x	x	x	x	x	x	x	x	x	x	x	x	x	x	061	-22	2.4
J	mid								x	x	x	x	x	x																					x	069	-26	4.3
	hih													x	x	x	x	x	x	x	x	x	x	x	x	x	x	x	x	x	x	x	x	x	x	061	-20	3.2
K	mos							x	x	x	x	x	x	x	x	x	x	x	x	x	x	x	x	x	x	x	x	x	x	x	x	x	x	x	x	073	-16	3.5
L	mos							x	x	x	x	x	x	x	x	x	x	x	x	x	x	x	x	x	x	x	x	x	x	x	x	x	x	x	x	065	-18	3.2

Sample	ID	NRM	LN2	100	198	300	350	400	450	481	500	520	541	550	555	560	565	570	575	580	585	590	595	600	615	635	650	662	670	675	680	685	690, 695, 700	Origin	Geographic Declination	Geographic Inclanation	MAD
A	mos						x	x	x	x	x	x	x	x	x	x	x	x	x	x	x	x	x	x	x									x	000	-49	1.5
B	mos				x	x	x	x	x	x	x	x	x	x	x	x	x	x	x	x	x	x	x	x	x									x	350	-49	1.9
C	mos						x	x	x	x	x	x	x	x	x	x	x	x	x	x	x	x	x	x	x									x	006	-44	2.2
D	mos				x	x	x	x	x	x	x	x	x	x	x	x	x	x	x	x	x	x	x	x	x									x	024	-42	2.3
E	mos				x	x	x	x	x	x	x	x	x	x	x	x	x	x	x	x	x	x	x	x	x	x	x	x	x					x	359	-51	3.5
F	mos					x	x	x	x	x	x	x	x	x	x	x	x	x	x	x	x	x	x	x	x	x	x	x	x					x	008	-46	2.7
G	mos						x	x	x	x	x	x	x	x	x	x	x	x	x	x	x	x	x	x	x	x	x	x	x	x	x	x	x	x	356	-50	2.9
H	mos						x	x	x	x	x	x	x	x	x	x	x	x	x	x	x	x	x	x	x	x	x	x	x	x	x			x	009	-49	2.5
I	mos				x	x	x	x	x	x	x	x	x	x	x	x	x	x	x	x	x	x	x	x	x	x	x	x	x	x	x	x		x	008	-51	2.7
J	all	x	x	x	x	x	x	x	x	x	x	x	x	x	x	x	x	x	x	x	x	x	x	x	x	x	x	x	x	x	x	x	x	x	360	-63	3.7
K	mos					x	x	x	x	x	x	x	x	x	x	x	x	x	x	x	x	x	x	x	x	x	x	x						x	355	-38	4.9
L	mos					x	x	x	x	x	x	x	x	x	x	x	x	x	x	x	x	x	x	x	x	x	x	x	x	x	x	x		x	357	-22	4.7
	low	x	x	x	x	x	x	x	x	x	x	x																							357	-53	2.9
	hih											x	x	x	x	x	x	x	x	x	x	x	x	x	x	x	x	x	x	x	x	x		x	357	-18	3.1
M	mos			x	x	x	x	x	x	x	x	x	x	x	x	x	x	x	x	x	x	x	x	x	x	x	x	x						x	005	15	3.8
N	mos							x	x	x	x	x	x	x	x	x	x	x	x	x	x	x	x	x	x	x	x							x	009	72	2.0
O	low				x	x	x	x	x	x	x	x	x																						227	-88	4.3
	hih												x	x	x	x	x	x	x	x	x	x	x	x	x									x	025	-34	6.1
P	mos	x	x	x	x	x	x	x	x	x	x	x	x	x	x	x	x	x	x	x	x	x												x	045	-02	4.3
Q	all	x	x	x	x	x	x	x	x	x	x	x	x	x	x	x	x	x	x	x	x	x	x											x	049	74	1.4
R	mos		x	x	x	x	x	x	x	x	x	x	x	x	x	x	x	x	x	x	x	x	x											x	094	-60	4.0
S	all	x	x	x	x	x	x	x	x	x	x	x	x	x	x	x	x	x	x	x	x	x												x	069	69	1.3
T	low	x	x	x	x	x	x	x	x																										357	-44	7.7
	hih								x	x	x	x	x	x	x	x	x	x	x	x	x	x	x	x	x	x	x	x						x	008	22	4.6
U	low	x	x	x	x	x	x	x	x	x	x	x	x	x	x	x	x	x	x	x															002	-25	3.5
	hih																			x	x	x	x	x	x	x	x	x						x	022	35	5.0
V	mos								x	x	x	x	x	x	x	x	x	x	x	x	x	x	x	x	x	x	x	x						x	003	17	4.3

Sample	ID	NRM	LN2	100	198	300	350	400	450	481	500	520	541	550	555	560	565	570	575	580	585	590	595	600	615	635	650	662	670	675	680	685	690, 695, 700	Origin	Geographic Declination	Geographic Inclanation	MAD
W	low	x	x	x	x	x	x	x	x	x																									041	-52	7.2
	mid									x	x	x	x	x	x	x	x	x																	351	01	9.1
	hih																	x	x	x	x	x	x	x	x	x	x	x	x	x	x			x	012	15	5.3
X	mos					x	x	x	x	x	x	x	x	x	x	x	x	x	x	x	x	x	x	x	x	x	x	x						x	005	26	2.6
Y	mos							x	x	x	x	x	x	x	x	x	x	x	x	x	x	x	x	x	x	x	x	x	x	x	x	x		x	007	27	3.8
Z	low					x	x	x	x																										309	-34	6.0
	hih								x	x	x	x	x	x	x	x	x	x	x	x	x	x	x	x	x	x	x	x	x	x	x	x	x	x	017	18	4.0

Sample	ID	NRM	LN2	100	198	300	350	400	450	481	500	520	541	550	555	560	565	570	575	580	585	590	595	600	605	610	615	635	origin	Geographic Declination	Geographic Inclanation	MAD	Comments
A	all	x	x	x	x	x	x	x	x	x	x	x	x	x	x	x	x	x	x	x	x	x	x	x	x	x	x	x	x	223	-44	4.3	lightning
B	all	x	x	x	x	x	x	x	x	x	x	x	x	x	x	x	x	x	x	x	x	x	x	x	x	x	x	x	x	240	-51	3.1	lightning
C	all	x	x	x	x	x	x	x	x	x	x	x	x	x	x	x	x	x	x	x	x	x	x	x	x	x	x	x	x	010	25	4.1	
D	all	x	x	x	x	x	x	x	x	x	x	x	x	x	x	x	x	x	x	x	x	x	x	x					x	014	15	5.2	
E	low	x	x	x	x	x	x	x	x	x	x	x																		004	-30	11.0	
	mid												x	x	x	x	x	x	x	x	x	x	x	x					x	004	19	2.3	
F	low		x	x	x	x	x	x	x	x	x	x	x	x	x															056	-14	17.9	
	mid														x	x	x	x	x	x	x	x	x	x					x	359	18	2.1	
G	mid											x	x	x	x	x	x	x	x	x	x	x	x	x					x	008	16	1.9	
H	mid											x	x	x	x	x	x	x	x	x	x	x	x	x					x	005	16	3.6	

Sample	ID	Line/Plane	NRM	LN2	100	200	300	350	400	450	481	500	520	540	550	555	560	565	570	575	581	585	591	595	origin	Geographic Declination	Geographic Inclanation	MAD	Comments
A	mi1	L					x	x	x	x	x	x	x													331	35	6.9	
	mi2	L											x	x	x	x	x	x	x	x	x	x	x	x		004	26	5.8	
	hpl	P											x	x	x	x	x	x	x	x	x	x	x	x	x	141	56	4.5	
	sep	L																				x	x	x	x	141	-33	6.4	
B	mos	L				x	x	x	x	x	x	x	x	x	x	x	x	x	x	x	x	x	x	x		323	65	5.8	
	hpl	P				x	x	x	x	x	x	x	x	x	x	x	x	x	x	x	x	x	x	x	x	055	01	9.2	
	sep	L																				x	x	x	x	150	-22	3.4	
C	low	L			x	x	x																			329	-39	13.9	
	mi2	L												x	x	x	x	x	x	x	x	x	x	x	x	026	21	2.4	
D	mi1	L				x	x	x	x	x	x	x	x	x	x											028	-52	5.6	
	mi2	L													x	x	x	x	x	x	x	x	x	x		026	-08	7.1	
	hpl	P													x	x	x	x	x	x	x	x	x	x	x	126	49	6.0	
	sep	L																			x	x	x	x	x	161	-35	2.2	
E	mi1	L			x	x	x	x																		356	-06	8.8	
	mi2	L							x	x	x	x	x	x	x	x	x	x	x	x	x	x	x	x		013	23	4.2	
	hpl	P							x	x	x	x	x	x	x	x	x	x	x	x	x	x	x	x	x	154	61	1.6	
	sep	L																					x	x	x	145	-29	1.3	
F	low	L	x	x	x	x																				014	-33	7.3	
	m12	L				x	x	x	x	x	x	x	x	x	x	x	x	x	x	x	x	x	x	x		031	07	8.9	
	hpl	P				x	x	x	x	x	x	x	x	x	x	x	x	x	x	x	x	x	x	x	x	135	64	6.7	
	sep	L																				x	x	x	x	179	-20	2.2	
G	low	L			x	x	x																			345	-73	14.8	
	sep	L								x	x	x	x	x	x	x	x	x	x	x	x	x	x	x	x	168	-40	2.3	
H	low	L	x	x	x	x	x	x				x	x	x	x	x	x	x	x							001	-39	13.7	
	m12	L						x	x	x	x	x	x	x	x	x	x	x	x	x	x	x	x	x		030	-05	12.2	
	hpl	P						x	x	x	x	x	x	x	x	x	x	x	x	x	x	x	x	x	x	116	44	7.1	
	sep	L																			x	x	x	x	x	162	-35	1.7	

Sample	ID	NRM	LN2	100	198	300	350	400	450	481	500	520	541	550	555	560	565	570	575	580	585	590	595	600	605	610	615	origin	Geographic Declination	Geographic Inclanation	MAD	Comments
A	mos			x	x	x	x	x	x	x	x	x	x	x	x	x	x	x	x	x	x	x	x	x				x	012	07	3.8	
B	all	x	x	x	x	x	x	x	x	x	x	x	x	x	x	x	x	x	x	x	x	x	x	x				x	006	05	3.2	
C	low				x	x	x	x																					014	-09	5.5	
	hih							x	x	x	x	x	x	x	x	x	x	x	x	x	x	x	x					x	031	21	4.5	
D	low				x	x	x	x																					348	-05	5.2	
	mid							x	x	x	x	x	x	x	x	x													134	-22	6.3	
	hih																	x	x	x	x	x	x	x	x			x	340	11	10.8	
E	low				x	x	x	x																					334	46	6.6	
	mid													x	x	x	x	x											168	40	7.6	
	hih																	x	x	x	x	x	x	x	x	x	x	x	351	25	6.9	
F	mid							x	x	x	x	x	x	x	x	x	x	x											176	07	5.8	
	hih																	x	x	x	x	x	x	x				x	358	24	5.5	
G	mid							x	x	x	x	x	x	x	x	x	x	x											163	-08	6.5	
	hih																	x	x	x	x	x	x	x	x	x		x	358	24	9.4	
H	mid										x	x	x	x	x	x	x	x											178	-18	4.2	
	hih																	x	x	x	x	x	x	x	x			x	349	26	11.6	
I	all	x	x	x	x	x	x	x	x	x	x	x	x	x	x	x	x	x	x	x	x	x	x					x	146	44	3.5	lightning
J	mid								x	x	x	x	x	x	x	x													145	-18	9.2	
	hih																		x	x	x	x	x					x	011	10	12.3	
K	mid					x	x	x	x	x	x	x	x	x	x	x	x	x											075	-49	8.2	
	hih																	x	x	x	x							x	010	06	10.8	

Table 2. Summary of paleomagnetic data from the Barby Formation, Sinclair region, Namibia.

Locality				Dyke/bed attitude			Present Coordinates						Tilt-Corrected			
Code	Lithology	Lat. (°S)	Long. (°E)	RHS (°)	Dip (°)	n/N	k	α95 (°)	D (°)	I (°)	VGP Lat. (°N)	VGP Long. (°E)	D (°)	I (°)	VGP Lat. (°N)	VGP Long. (°E)
Westernmost locality																
JP1101	dyke	25.7250	016.5788			4/6		11.9	183.7	04.8			-----	-----	-----	-----
	Barby-contact	25.7249	016.5787			3/10		39.6	184.4	-49.4			-----	-----	-----	-----
	Barby-hybrid	25.7249	016.5787			1/10		-----	061.5	-36.6			069.5	-07.9	-----	-----
	Barby-host	25.7249	016.5787			6/10		13.7	048.6	-11.1			048.7	10.9		
JP1202	Barby-host	25.7243	016.5782			8/8		7.6	050.7	-17.1	39.1	096.6	052.8	07.3	31.1	84.7
West-central locality																
JP1102	dyke1	25.7257	016.5959			8/8		5.9	009.8	-43.0	81.1	104.2	-----	-----	-----	-----
JP1203	Barby-contact1	25.7259	016.5959			9/15	91.1	5.1	017.4	-45.4	74.4	114.8	-----	-----	-----	-----
	Barby-host	25.7259	016.5961			3/15	58.9	16.2	062.7	-07.1	26.1	097.5	060.9	26.3	18.7	080.2
	Barby-contact2	25.7259	016.5962			6/15	28.8	11.6	002.2	-39.9	86.4	050.7	-----	-----	-----	-----
JP1204	dyke2	25.7256	016.5962			8/8		3.6	014.2	-42.0	77.1	103.2	-----	-----	-----	-----
JP1205	Barby-contact2	25.7256	016.5962			5/17	38.6	9.9	011.4	-39.8	79.2	092.5	-----	-----	-----	-----
	Barby-host	25.7257	016.5964			12/17	81.4	4.8	061.4	-15.5	29.1	101.2	061.2	17.8	21.1	084.6
JP1206	dyke3	25.7259	016.5968			8/8		7.2	017.5	-30.4	71.2	080.2	-----	-----	-----	-----
JP1207	Barby-contact3	25.7259	016.5968			5/12	30.7	12.5	020.2	-18.3	64.8	069.8	-----	-----	-----	-----
	Barby-hybrid	25.7259	016.5968			1/12	-----	-----	048.9	-27.0	-----	-----	-----	-----	-----	-----
	Barby-host	25.7260	016.5967			9/12	242	3.3	065.0	-20.5	27.0	105.7	065.5	13.8	18.5	088.9
Central locality																
JP1103-04	dyke-lightning					N/A		N/A	N/A	N/A	N/A	N/A	-----	-----	-----	-----
JP1208	Barby-NU					11/26	74.0	5.1	003.4	-48.6			028.6	-29.5		
	Barby-hybrid					1/26	-----	-----	356.6	-18.1	-----	-----	-----	-----	-----	-----
	Barby-ND					7/26	63.3	7.1	010.6	23.0			351.9	33.4		
Eastern locality																

JP1218	Barby-ND	6/8	148.5	5.0	006.8	18.1			356.7	-38.6		
JP1219	dyke-ND	6/8	21.9	13.3	022.1	13.6			-----	-----	-----	-----
	dyke-SE	7/8	28.5	10.6	157.6	-31.2			-----	-----	-----	-----
JP1220	Barby-ND	10/11	21.7	10.0	002.7	16.2			-----	-----	-----	-----
	Barby-SE	6/11	06.7	25.2	160.8	-03.9			-----	-----	-----	-----
Mean	Barby-host	2 sites	95.8	25.8	056.8	-16.8	33.5	099.7	057.7	12.4	25.5	085.2
Mean	Barby-ND	3 sites	251.0	7.8	006.6	19.1	53.8	027.9	-----	-----	-----	-----
Mean	Barby-SE	2 sites	17.5	63.8	159.3	-17.6	49.5	344.1	-----	-----	-----	-----

K=xx.x A95=xx.x°

Notes: RHS = Right-hand strike. Strat=thickness of sampled section. n/N = number of specimens included in the mean / number of specimens analyzed. D = mean declination. I = mean inclination. k,K = Fisher's (1953) precision parameter. α95, A95 = radius of the 95% confidence cone. VGP = virtual geomagnetic pole (inverted to Northern Hemisphere as needed).
* Mean includes data from both polarities, inverted as necessary.